

Three-particle correlations in QCD jets and beyond

Redamy Pérez-Ramos ¹, Vincent Mathieu ² and Miguel-Angel Sanchis-Lozano ³

Departament de Física Teòrica and IFIC, Universitat de València - CSIC

Dr. Moliner 50, E-46100 Burjassot, Spain

Abstract: In this paper, we present a more detailed version of our previous work for three-particle correlations in quark and gluon jets [1]. We give theoretical results for this observable in the double logarithmic approximation and the modified leading logarithmic approximation. In both resummation schemes, we use the formalism of the generating functional and solve the evolution equations analytically from the steepest descent evaluation of the one-particle distribution. In addition, in this paper we include predictions beyond the limiting spectrum approximation and study this observable near the hump of the single inclusive distribution. We thus provide a further test of the local parton hadron duality (LPHD) and make predictions for the LHC. The computation of higher rank correlators is presented in the double logarithmic approximation and shown to be rather cumbersome.

¹e-mail: redamy.perez@uv.es

²e-mail: vincent.mathieu@ific.uv.es

³e-mail: miguel.angel.sanchis@ific.uv.es

1 Introduction

The observation of quark and gluon jets has played a crucial role in establishing Quantum Chromodynamics (QCD) as the theory of strong interaction within the Standard Model of particle physics [2, 3]. Jets, narrowly collimated bundles of hadrons, reflect configurations of quarks and gluons at short distances [4, 5].

The evolution of gluon and quark initiated jets is dominated by soft gluon bremsstrahlung. Powerful schemes, like the Double Logarithmic Approximation (DLA) and the Modified Leading Logarithmic Approximation (MLLA), which allow for the perturbative resummation of soft-collinear and hard-collinear gluons before the hadronization occurs, have been developed over the past thirty years (for a review see [6]). In the frame of high energy jets, one of the striking predictions of perturbative QCD (pQCD), which follows as a consequence of Angular Ordering (AO) within the MLLA and the Local Parton Hadron Duality (LPHD) hypothesis [7], is the existence of the hump-backed shape [8] of the inclusive energy distribution of hadrons, later confirmed by experiments at colliders like the LEP [9, 10] and the Tevatron [11]. Within the same formalism, the transverse momentum distribution, or k_\perp -spectra of hadrons produced in $p\bar{p}$ collisions at center of mass energy $\sqrt{s} = 1.96$ TeV at the Tevatron [12], was well described by MLLA [13] and next-to-MLLA (NMLLA) [14, 15] predictions inside the validity ranges provided by such schemes, both supported by the LPHD. Thus, the study and tests of enough inclusive observables like the inclusive energy distribution and the inclusive transverse momentum k_\perp spectra of hadrons have shown that the perturbative stage of the process, which evolves from the hard scale or leading parton virtuality $Q \sim E$ to the hadronization scale Q_0 , is dominant. In particular, these issues suggest that the hadronization stage of the QCD cascade do not affect pQCD predictions and therefore, that the LPHD hypothesis is successful while treating one-particle inclusive observables.

The study of particle correlations in intrajet cascades, which are less inclusive observables, provide a refined test of the partonic dynamics and the LPHD. In [16], the two-particle correlations inside quark and gluon jets were first computed at DLA. In [17, 18], this observable was computed for the first time at MLLA for such particles, whose energy or x (energy fraction of the jet carried away by one parton) stays close to the maximum of the one-particle distribution. In [19], the previous solutions were extended, at MLLA, to all possible values of x by exactly solving the QCD evolution equations. This observable was measured by the OPAL collaboration in the e^+e^- annihilation at the Z^0 peak, that is for $\sqrt{s} = 91.2$ GeV at LEP [20]. Though the agreement with predictions presented in [19] turned out to be rather good for the description of the data [20], a discrepancy still subsists pointing out a possible failure of the LPHD for less inclusive observables. However, these measurements were redone by the CDF collaboration in $p\bar{p}$ collisions at the Tevatron for mixed samples of quark and gluon jets [11]. The agreement with predictions presented in [17, 18] turned out to be rather good, in particular for very soft particles ($x \ll 0.1$) having very close energy fractions ($x_1 \approx x_2$). A discrepancy between the OPAL and CDF analysis showed up and still stays unclear. That is why, the measurement of two-particle correlations at the LHC becomes crucial.

By going one step beyond, in this paper we give predictions for three-particle correlations inside quark and gluon jets. This observable together with two-particle correlations can be measured in equal footing at the LHC. Such tests will provide further verifications of the LPHD for less inclusive observables and shed more light on the role of confinement in jet evolution. Further issues on the importance of

correlations versus single-particle distributions studies have been presented in [21, 22].

The paper is organized as follows.

- in section 2 we recall the formalism of jet generating functionals and their evolution equations;
- the kinematics and the process for the inclusive production of three particles inside the jet are specified in subsection 2.1 and 2.1.1 respectively;
- in subsection 2.2, we obtain the MLLA exact system of integro-differential evolution equations for the three-particle correlations and in subsection 2.3, the single logarithms (SLs) contributions are obtained from the exact evolution equations;
- in subsection 2.4, we obtain the DLA solution of the evolution equations and study the shape and overall normalization of this observable;
- in subsection 2.5 the evolution equations are solved iteratively and the solution are expressed in terms of the logarithmic derivatives of the one-particle distribution and the two-particle correlations;
- in subsection 2.6, we finally give the analytical predictions which will be displayed in order to provide predictions for the Tevatron and the LHC;
- in subsection 2.7, the hump approximation is applied to this observable;
- in subsection 2.8, the region in x where the emission of three correlated particles becomes dominant is discussed;
- in subsection 2.9, we give the analytical solution of the DLA four-particle correlator and show that including higher order corrections for differential higher rank correlators would become a cumbersome task;
- in subsection 3, the predictions are displayed and the phenomenology is applied to the Tevatron and the LHC;
- a conclusion summarizes this work; the appendices are written as complements of the main core of the paper.

2 Formalism of the generating functional

A generating functional $Z(E, \Theta; \{u\})$ can be constructed [23] that describes the azimuth averaged parton content of a jet of energy E with a given opening half-angle Θ ; by virtue of the exact angular ordering (MLLA), it satisfies the following integro-differential evolution equation [6]

$$\frac{d}{d \ln \Theta} Z_A(p, \Theta; \{u\}) = \frac{1}{2} \sum_{B,C} \int_0^1 dz \Phi_A^{B[C]}(z) \frac{\alpha_s(k_\perp^2)}{\pi} \left(Z_B(zp, \Theta; \{u\}) Z_C((1-z)p, \Theta; \{u\}) - Z_A(p, \Theta; \{u\}) \right); \quad (1)$$

in (1), z and $(1 - z)$ are the energy-momentum fractions carried away by the two offspring in the $A \rightarrow BC$ parton decay described by the standard one loop splitting functions [24]

$$\Phi_q^{g[q]}(z) = C_F \frac{1 + z^2}{1 - z}, \quad \Phi_q^{g[\bar{q}]}(z) = C_F \frac{1 + (1 - z)^2}{z}, \quad (2)$$

$$\Phi_g^{g[\bar{q}]}(z) = T_R (z^2 + (1 - z)^2), \quad \Phi_g^{g[g]}(z) = 2C_A \left(\frac{1 - z}{z} + \frac{z}{1 - z} + z(1 - z) \right), \quad (3)$$

$$C_A = N_c, \quad C_F = (N_c^2 - 1)/2N_c, \quad T_R = 1/2, \quad (4)$$

where N_c is the number of colors; Z_A in the integral in the r.h.s. of (1) accounts for 1-loop virtual corrections, which exponentiate into Sudakov form factors. $\alpha_s(q^2)$ is the running coupling constant of QCD

$$\alpha_s(q^2) = \frac{4\pi}{4N_c\beta_0 \ln \frac{q^2}{\Lambda_{QCD}^2}}, \quad (5)$$

where $\Lambda_{QCD} \approx$ a few hundred MeV's is the intrinsic scale of QCD, and

$$\beta_0 = \frac{1}{4N_c} \left(\frac{11}{3}N_c - \frac{4}{3}n_f T_R \right) \quad (6)$$

is the first term in the perturbative expansion of the β function, n_f the number of light quark flavors.

If the radiated parton with 4-momentum $k = (k_0, \vec{k})$ is emitted with an angle Θ with respect to the direction of the jet, one has (k_\perp is the modulus of the transverse trivector \vec{k}_\perp orthogonal to the direction of the jet) $k_\perp \simeq |\vec{k}|\Theta \approx k_0\Theta \approx zE\Theta$ when $z \ll 1$ or $k_\perp \approx (1 - z)E\Theta$ when $z \rightarrow 1$, and a collinear cutoff $k_\perp \geq Q_0$ is imposed.

In (1) the symbol $\{u\}$ denotes a set of *probing functions* $u_a(k)$ with k the 4-momentum of a secondary parton of type a . The jet functional is normalized to the total jet production cross section such that

$$Z_A(p, \Theta; u \equiv 1) = 1; \quad (7)$$

for vanishingly small opening angle it reduces to the probing function of the single initial parton

$$Z_A(p, \Theta \rightarrow 0; \{u\}) = u_A(k \equiv p). \quad (8)$$

To obtain *exclusive* n -particle distributions one takes n variational derivatives of Z_A over $u(k_i)$ with appropriate particle momenta, $i = 1 \dots n$, and sets $u \equiv 0$ afterwards; *inclusive* distributions are generated by taking variational derivatives around $u \equiv 1$. We introduce the n -particle differential inclusive distribution, also known as parton densities, as [6]

$$x_1 \dots x_n D_A^{(n)}(x_1, \dots, x_n, Y) = E_1 \dots E_n \frac{\delta^n}{\delta u(k_1) \dots \delta u(k_n)} Z_A(k_1, \dots, k_n, \Theta; \{u(k)\}) \Big|_{u=1}. \quad (9)$$

Accordingly, we introduce the following notations for gluon and quark jets $A = G, Q, \bar{Q}$

$$A_{1\dots n}^{(n)}(z) \equiv \frac{x_1}{z} \dots \frac{x_n}{z} D_A^{(n)}\left(\frac{x_1}{z}, \dots, \frac{x_n}{z}, Y + \ln z\right), \quad A_{1\dots n}^{(n)} \equiv x_1 \dots x_n D_A^{(n)}(x_1, \dots, x_n, Y), \quad (10)$$

which we will use hereafter; x_i corresponds to the Feynman energy fraction of the jet taken away by one particle “ i ”. In the case of three-particle correlations $n = 3$, the observable to be measured experimentally reads

$$C_{A_{123}}^{(3)} = \frac{A_{123}^{(3)}}{A_1 A_2 A_3}.$$

2.1 Kinematics and variables

The probability of soft gluon radiation off a color charge (moving in the z direction) has the polar angle dependence

$$\frac{\sin \Theta d\Theta}{2(1 - \cos \Theta)} = \frac{d \sin(\Theta/2)}{\sin(\Theta/2)} \simeq \frac{d\Theta}{\Theta};$$

therefore, we choose the angular evolution parameter to be

$$Y = \ln \frac{2E \sin(\Theta/2)}{Q_0} \Rightarrow dY = \frac{d \sin(\Theta/2)}{\sin(\Theta/2)}; \quad (11)$$

note that this choice accounts for finite angles $\mathcal{O}(1)$ up to the full opening half-angle $\Theta = \pi$, at which

$$Y_{\Theta=\pi} = \ln \frac{2E}{Q_0},$$

where $2E$ is the center-of-mass annihilation energy of the process $e^+e^- \rightarrow q\bar{q}$. For small angles (11) reduces to

$$Y \simeq \ln \frac{Q}{Q_0}, \quad \Theta \ll 1, \quad \frac{d}{dY} = \frac{d}{d \ln \Theta}, \quad (12)$$

where $Q = E\Theta$, defined as the virtuality of the jet, is the maximal transverse momentum of a parton inside the jet with opening half-angle Θ . Moreover, we make use of variables known from previous works [19, 25],

$$\ell = \ln \frac{z}{x_i}, \quad y = \ln \frac{x_j E \Theta_1}{Q_0}, \quad \lambda = \frac{Q_0}{\Lambda_{QCD}}, \quad (13)$$

$$\ell_i = \ln \frac{1}{x_i}, \quad y_j = \ln \frac{x_j E \Theta_0}{Q_0}, \quad \eta_{ij} = \ln \frac{x_i}{x_j}, \quad Y = \ell_i + y_j + \eta_{ij}. \quad (14)$$

Since $\frac{d}{dy} = \frac{d}{d \ln \Theta_1}$, y could also be used as the evolution-time variable in forthcoming quark and gluon jet evolution equations. Accordingly, the anomalous dimension, related to the coupling constant (5), can be parametrized as follows

$$\gamma_0^2(q^2) = 2N_c \frac{\alpha_s(q^2)}{\pi} \Rightarrow \gamma_0^2(\ell + y) = \frac{1}{\beta_0(\ell + y + \eta_{ij} + \lambda)}, \quad (15)$$

such that,

- for one particle [6], the denominator in (15) is simply $\ell + y + \lambda$, with [26] $\ell = \ln \frac{z}{x}$, $y = \ln \frac{x E \Theta}{Q_0}$, $\eta = 0$;
- for two-particle correlation [19, 25], $\ell + y + \eta_{12}$, with $\ell = \ln \frac{z}{x_1}$, $y = \ln \frac{x_2 E \Theta_1}{Q_0}$, $\eta_{12} = \ln \frac{x_1}{x_2}$;
- for three-particle correlation, $\ell + y + \eta_{13}$, with $\ell = \ln \frac{z}{x_1}$, $y = \ln \frac{x_3 E \Theta_1}{Q_0}$, $\eta_{13} = \eta_{12} + \eta_{23} = \ln \frac{x_1}{x_3}$.

2.1.1 Integration bounds for three-particle evolution equations

The production of three hadrons is displayed in Fig.1 after a quark or a gluon (A) jet of energy E , half opening angle Θ_0 and virtuality $Q = E\Theta_0$ has been produced in a high energy collision. The kinematical variable characterizing the process is given by the transverse momentum $k_\perp = zE\Theta_1 \geq Q_0$ (or $(1 - z)E\Theta_1 \geq Q_0$) of the first splitting $A \rightarrow BC$. The parton C fragments into three offspring such

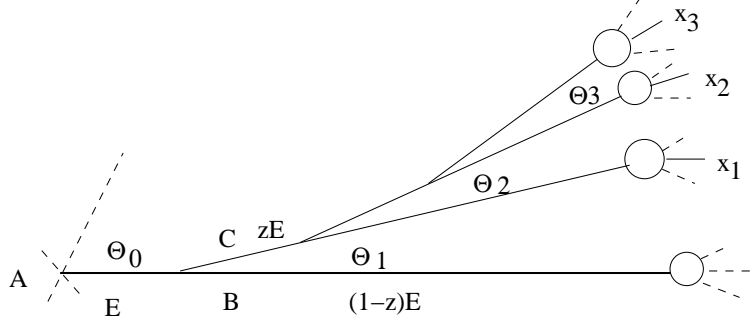


Figure 1: Three-particle yield and angular ordering inside a high energy jet.

that three hadrons of energy fractions x_1 , x_2 and x_3 can be triggered from the same cascade following the condition:

$$\Theta_0 \geq \Theta_1 \geq \Theta_2 \geq \Theta_3, \quad (16)$$

which arises from the exact AO in MLLA [6]. In particular, the condition $\Theta_0 \geq \Theta_1$ is kinematical rather than supported by the AO; it states that every collinear gluon is emitted inside the jet of half opening angle Θ_0 . The two variables entering the evolution equations are z and Θ_1 , such that

$$x_1 \leq z \leq 1 \quad \Rightarrow \quad 0 \leq \ell \leq \ell_1. \quad (17)$$

From (16) and the initial condition at threshold $x_3 E \Theta_0 \geq x_3 E \Theta_1 \geq x_3 E \Theta_3 \geq Q_0$, one has

$$\frac{Q_0}{x_3 E} \leq \Theta_1 \leq \Theta_0 \quad \Rightarrow \quad 0 \leq y \leq y_3. \quad (18)$$

2.2 From single inclusive distribution and two-particle correlation to three-particle correlation

The evolution equations satisfied by (9) are derived from the MLLA master equation for the generating functional $Z_A(u(k_i))$ (1). In this case, one takes the first $\frac{\delta Z_A}{\delta u(k_1)}$, second $\frac{\delta^2 Z_A}{\delta u(k_1) \delta u(k_2)}$, and finally third $\frac{\delta^3 Z_A}{\delta u(k_1) \dots \delta u(k_3)}$ functional derivatives of $Z_A(u(k_i))$ over the probing functions $u(k_i)$ so as to obtain the system of evolution equations for 3-particle correlations. Following from (1), after applying the operator $\frac{\delta^3}{\delta u(k_1) \dots \delta u(k_3)}$ to both members of the equation, according to (9) and (10) together with the initial condition (7), it is straightforward to get the coupled system of evolution equations

$$Q_y^{(3)} = \int_{x_1}^1 dz \frac{\alpha_s}{\pi} \Phi_g^g(z) \left[G^{(3)}(z) + \left(Q^{(3)}(1-z) - Q^{(3)} \right) + G_{12}^{(2)}(z) Q_3(1-z) + G_3(z) Q_{12}^{(2)} \right. \\ \left. + G_{13}^{(2)}(z) Q_2(1-z) + G_2(z) Q_{13}^{(2)} + G_{23}^{(2)}(z) Q_1(1-z) + G_1(z) Q_{23}^{(2)} \right], \quad (19a)$$

$$G_y^{(3)} = \int_{x_1}^1 dz \frac{\alpha_s}{\pi} \Phi_g^g(z) \left[G^{(3)}(z) - z G^{(3)} + G_{12}^{(2)}(z) G_3(1-z) + G_{13}^{(2)}(z) G_2(1-z) \right. \\ \left. + G_{23}^{(2)}(z) G_1(1-z) \right] + \int_{x_1}^1 dz \frac{\alpha_s}{\pi} n_f \Phi_g^q(z) \left[\left(2Q^{(3)}(z) - G^{(3)} \right) + 2Q_{12}^{(2)}(z) Q_3(1-z) \right. \\ \left. + 2Q_{13}^{(2)}(z) Q_2(1-z) + 2Q_{23}^{(2)}(z) Q_1(1-z) \right]. \quad (19b)$$

The l.h.s. of the equations (19a) and (19b) can be written in the convenient form

$$\hat{A}^{(3)} = A^{(3)} - A_1 A_2 A_3 - (A_{12}^{(2)} - A_1 A_2) A_3 - (A_{13}^{(2)} - A_1 A_3) A_2 - (A_{23}^{(2)} - A_2 A_3) A_1, \quad (20)$$

where $A = G, Q, \bar{Q}$ is the leading parton of the jet. Moreover, we have introduced the notations $A_{1\dots n}^{(n)} = A_{1\dots n}^{(n)}(1)$, where

$$A_{1\dots n}^{(n)} \equiv A_{1\dots n}^{(n)}(1) = x_1 \dots x_n D^{(n)}(x_1, \dots, x_n, Y),$$

for the sake of simplicity. The evolution equations for the single inclusive distribution and the two-particle correlation are written in [19] in the form

$$Q_y = \int_{x_1}^1 dz \frac{\alpha_s}{\pi} \Phi_q^g(z) \left[(Q(1-z) - Q) + G(z) \right], \quad (21a)$$

$$G_y = \int_{x_1}^1 dz \frac{\alpha_s}{\pi} \left[\Phi_g^g(z) (G(z) - zG) + n_f \Phi_g^q(z) (2Q(z) - G) \right], \quad (21b)$$

and

$$(Q^{(2)} - Q_1 Q_2)_y = \int_{x_1}^1 dz \frac{\alpha_s}{\pi} \Phi_q^g(z) \left[G^{(2)}(z) + (Q^{(2)}(1-z) - Q^{(2)}) \right. \\ \left. + (G_1(z) - Q_1) (Q_2(1-z) - Q_2) + (G_2(z) - Q_2) (Q_1(1-z) - Q_1) \right], \quad (22a)$$

$$(G^{(2)} - G_1 G_2)_y = \int_{x_1}^1 dz \frac{\alpha_s}{\pi} \Phi_g^g(z) \left[(G^{(2)}(z) - zG^{(2)}) + (G_1(z) - G_1) (G_2(1-z) - G_2) \right] \\ + \int_{x_1}^1 dz \frac{\alpha_s}{\pi} n_f \Phi_g^q(z) \left[2(Q^{(2)}(z) - Q_1(z) Q_2(z)) - (G^{(2)} - G_1 G_2) \right. \\ \left. + (2Q_1(z) - G_1) (2Q_2(1-z) - G_2) \right], \quad (22b)$$

respectively. Making use of the equations (21a,21b) and (22a,22b), one can then construct the total derivatives $[A_1 A_2 A_3]_y$, $[(A_{12}^{(2)} - A_1 A_2) A_3]_y$, $[(A_{13}^{(2)} - A_1 A_3) A_2]_y$, $[(A_{23}^{(2)} - A_2 A_3) A_1]_y$ as they appear in (20), which are to be subtracted, term by term from the system of equations (19a,19b). Therefore, we get the equivalent system for the three-particle correlations inside quark and gluon jets:

$$\hat{Q}_y^{(3)} = \int_{x_1}^1 dz \frac{\alpha_s}{\pi} \Phi_q^g(z) \left[G^{(3)}(z) + (Q^{(3)}(1-z) - Q^{(3)}) \right. \\ + (Q_{12}^{(2)}(1-z) - Q_{12}^{(2)}) (G_3(z) - Q_3) + (G_{12}^{(2)}(z) - Q_{12}^{(2)}) (Q_3(1-z) - Q_3) \\ + (Q_{13}^{(2)}(1-z) - Q_{13}^{(2)}) (G_2(z) - Q_2) + (G_{13}^{(2)}(z) - Q_{13}^{(2)}) (Q_2(1-z) - Q_2) \\ + (Q_{23}^{(2)}(1-z) - Q_{23}^{(2)}) (G_1(z) - Q_1) + (G_{23}^{(2)}(z) - Q_{23}^{(2)}) (Q_1(1-z) - Q_1) \\ + ((Q_1 - G_1(z)) (Q_2(1-z) - Q_2) + (Q_2 - G_2(z)) (Q_1(1-z) - Q_1)) Q_3 \\ + ((Q_1 - G_1(z)) (Q_3(1-z) - Q_3) + (Q_3 - G_3(z)) (Q_1(1-z) - Q_1)) Q_2 \\ \left. + ((Q_2 - G_2(z)) (Q_3(1-z) - Q_3) + (Q_3 - G_3(z)) (Q_2(1-z) - Q_2)) Q_1 \right], \quad (23a)$$

$$\hat{G}_y^{(3)} = \int_{x_1}^1 dz \frac{\alpha_s}{\pi} \Phi_g^g(z) \left[(G^{(3)}(z) - zG^{(3)}) + (G_{12}^{(2)}(z) - G_{12}^{(2)}) (G_3(1-z) - G_3) \right. \\ + (G_{13}^{(2)}(z) - G_{13}^{(2)}) (G_2(1-z) - G_2) + (G_{23}^{(2)}(z) - G_{23}^{(2)}) (G_1(1-z) - G_1) \\ + (G_1 - G_1(z)) (G_2(1-z) - G_2) G_3 + (G_1 - G_1(z)) (G_3(1-z) - G_3) G_2 \\ + (G_2 - G_2(z)) (G_3(1-z) - G_3) G_1 \left. + \int_{x_1}^1 dz \frac{\alpha_s}{\pi} n_f \Phi_g^q(z) \left[(2Q^{(3)}(z) - G^{(3)}) \right. \right. \\ + 2(Q_{12}^{(2)}(z) - G_{12}^{(2)}) (Q_3(1-z) - G_3) + (2Q_1(z) Q_2(z) - G_1 G_2) G_3 \\ \left. \left. + 2(Q_{13}^{(2)}(z) - G_{13}^{(2)}) (Q_2(1-z) - G_2) + (2Q_1(z) Q_3(z) - G_1 G_3) G_2 \right] \right] \quad (23b)$$

$$\begin{aligned}
& + 2 \left(Q_{23}^{(2)}(z) - G_{23}^{(2)} \right) (Q_1(1-z) - G_1) + (2Q_2(z)Q_3(z) - G_2G_3)G_1 \\
& + (G_1 - 2Q_1(z))(2Q_2(1-z) - G_2)G_3 + (G_1 - 2Q_1(z))(2Q_3(1-z) - G_3)G_2 \\
& + (G_2 - 2Q_2(z))(2Q_3(1-z) - G_3)G_1].
\end{aligned}$$

The system of evolution equations (23a,23b), which appears as a consequence of the exact AO in intra-jet cascades, provides the complete theoretical picture of the three-particle correlations as a function of x_i and the characteristic hardness of the jet Q ; this is the first new result of this paper. However, since these equations could only be solved numerically, we will extract the SLs contributions $\mathcal{O}(\sqrt{\alpha_s})$ in order to provide an approximated analytical solution in the following.

2.3 Approximate evolution equations

Let us start with equation (23a). We proceed to cast all SLs contributions corresponding to hard-collinear parton splittings in the shower. In the hard parton fragmentation region one has $z \sim (1-z) \sim 1$, such that the second contribution in (23a) can be approximated through a Taylor series for $\ln z \sim \ln(1-z) \ll \ell_1$, written in the appendix A. Therefore, one obtains the simplified system of evolution equations

$$\hat{Q}_y^{(3)} = \int_{x_1}^1 dz \frac{\alpha_s}{\pi} \Phi_q^g(z) G^{(3)}(z), \quad (24)$$

$$\begin{aligned}
\hat{G}_y^{(3)} = & \int_{x_1}^1 dz \frac{\alpha_s}{\pi} (1-z) \Phi_g^g(z) G^{(3)}(z) + \int_{x_1}^1 dz \frac{\alpha_s}{\pi} n_f \Phi_g^q(z) \left[\left(2Q^{(3)} - G^{(3)} \right) + 2 \left(Q_{12}^{(2)} - G_{12}^{(2)} \right) \right. \\
& \times (Q_3 - G_3) + (2Q_1Q_2 - G_1G_2)G_3 + 2 \left(Q_{13}^{(2)} - G_{13}^{(2)} \right) (Q_2 - G_2) + (2Q_1Q_3 - G_1G_3)G_2 \\
& + 2 \left(Q_{23}^{(2)} - G_{23}^{(2)} \right) (Q_1 - G_1) + (2Q_2Q_3 - G_2G_3)G_1 + (G_1 - 2Q_1)(2Q_2 - G_2)G_3 \\
& \left. + (G_1 - 2Q_1)(2Q_3 - G_3)G_2 + (G_2 - 2Q_2)(2Q_3 - G_3)G_1 \right],
\end{aligned} \quad (25)$$

where we have kept all terms of order $\mathcal{O}(\sqrt{\alpha_s})$, which contribute to MLLA. In addition, from the DLA relation $Z_A = Z_G^{C_A/N_c}$ [27], and Eqs.(9-10), one has the useful expressions for the single inclusive distribution, two- and three-particle correlations:

$$Q_i = \frac{C_F}{N_c} G_i, \quad Q_{ij}^{(2)} = \frac{C_F}{N_c} G_{ij}^{(2)} + \frac{C_F}{N_c} \left(\frac{C_F}{N_c} - 1 \right) G_i G_j, \quad i \neq j, \quad (26)$$

$$\begin{aligned}
Q^{(3)} = & \frac{C_F}{N_c} G^{(3)} + \frac{C_F}{N_c} \left(\frac{C_F}{N_c} - 1 \right) \left(G_{12}^{(2)} G_3 + G_{13}^{(2)} G_2 + G_{23}^{(2)} G_1 \right) + \frac{C_F}{N_c} \left(\frac{C_F}{N_c} - 1 \right) \left(\frac{C_F}{N_c} - 2 \right) \\
& \times G_1 G_2 G_3,
\end{aligned} \quad (27)$$

which in turn can be replaced in (25). The two expressions written in (26) are known from previous works at DLA [16, 27], while (27) will be used for the first time in this context. After integrating over the regular part of the splitting functions (2), (3) and (4), one obtains the integro-differential system of equations ($\eta_{13} = \eta_{12} + \eta_{23}$),

$$\hat{Q}_y^{(3)} = \frac{C_F}{N_c} \int_0^{\ell_1} d\ell \gamma_0^2(\ell + y_3) G^{(3)}(\ell, y_3; \eta_{13}) - \frac{3}{4} \frac{C_F}{N_c} \gamma_0^2(\ell_1 + y_3) G^{(3)}(\ell_1, y_3; \eta_{13}), \quad (28)$$

$$\begin{aligned}
\hat{G}_y^{(3)} = & \int_0^{\ell_1} d\ell \gamma_0^2(\ell + y_3) G^{(3)}(\ell, y_3; \eta_{13}) - a \gamma_0^2(\ell_1 + y_3) G^{(3)}(\ell_1, y_3; \eta_{13}) + (a - b) \gamma_0^2(\ell_1 + y_3) \\
& \times \left[\left(G_{12}^{(2)}(\ell_1, y_3 + \eta_{23}; \eta_{12}) - G_1(\ell_1, y_3 + \eta_{13}) G_2(\ell_1 + \eta_{12}, y_3 + \eta_{23}) \right) G_3(\ell_1 + \eta_{13}, y_3) \right. \\
& \left. + \left(G_{13}^{(2)}(\ell_1, y_3; \eta_{13}) - G_1(\ell_1, y_3 + \eta_{13}) G_3(\ell_1 + \eta_{13}, y_3) \right) G_2(\ell_1 + \eta_{12}, y_3 + \eta_{23}) \right]
\end{aligned} \quad (29)$$

$$\begin{aligned}
& + \left(G_{23}^{(2)}(\ell_1 + \eta_{12}, y_3; \eta_{23}) - G_2(\ell_1 + \eta_{12}, y_3 + \eta_{23}) G_3(\ell_1 + \eta_{13}, y_3) \right) G_1(\ell_1, y_3 + \eta_{13}) \Big] \\
& + (a - c) \gamma_0^2 (\ell_1 + y_3) G_1(\ell_1, y_3 + \eta_{13}) G_2(\ell_1 + \eta_{12}, y_3 + \eta_{23}) G_3(\ell_1 + \eta_{13}, y_3),
\end{aligned}$$

with the following hard constants,

$$a(n_f) = \frac{1}{4N_c} \left[\frac{11}{3} N_c + \frac{4}{3} n_f T_R \left(1 - 2 \frac{C_F}{N_c} \right) \right] \stackrel{n_f=3}{=} 0.935, \quad (30)$$

$$b(n_f) = \frac{1}{4N_c} \left[\frac{11}{3} N_c - \frac{4}{3} n_f T_R \left(1 - 2 \frac{C_F}{N_c} \right)^2 \right] \stackrel{n_f=3}{=} 0.915, \quad (31)$$

$$c(n_f) = \frac{1}{4N_c} \left[\frac{11}{3} N_c + \frac{4}{3} n_f T_R \left(1 - 2 \frac{C_F}{N_c} \right)^3 \right] \stackrel{n_f=3}{=} 0.917, \quad (32)$$

where $n_f = 3$ corresponds to the number of light active flavors of quarks u, d, s . As an example of such procedure, one could write the example,

$$a(n_f) = \int_0^1 dz \left[(1-z) \left(2 - z(1-z) \right) + \frac{n_f T_R}{2C_A} \left(z^2 + (1-z)^2 \right) \left(1 - 2 \frac{C_F}{N_c} \right) \right].$$

The first integral terms of the equations in (28) and (29) are of classical origin and therefore, universal. Corrections $\propto -\frac{3}{4}$, a , $(a - b)$ and $(a - c)$, which are $\mathcal{O}(\sqrt{\alpha_s})$ suppressed, better account for energy conservation at each vertex of the splitting process, as compared with the DLA. Notice that the form of the quark initiated jet equation (28) is universal at MLLA (see (80) and (82 in the appendix A.1 for the single inclusive distribution and two-particle correlation respectively), that is, invariant with respect to the number of particles considered in the cascade. In the equation for the gluon initiated jet (29), the first and second constants $a(n_f)$ and $b(n_f)$ were obtained in the frame of the single inclusive distribution and two-particle correlations respectively [17, 18]. The third constant $c(n_f)$ appears in this paper for the first time for the three-particle correlation. In particular, notice that a certain recurrency shows up in the coefficients combining the colour factors $(-1)^{n-1} \left(1 - 2 \frac{C_F}{N_c} \right)^n$, as a function of the number n of particles considered in the shower.

2.4 DLA solution of the evolution equations

In this subsection we compute the leading order DLA contributions in order to provide general features concerning the the shape and overall normalization of three-particle correlations. This procedure is equivalent to cast the leading order (LO) solution of the equations (28,29). We differentiate (28) and (29) with respect to “ ℓ ”, such that after setting hard corrections $\propto 3/4$, $a, b, c = 0$, the MLLA evolution equations are reduced to the new DLA compact differential equation

$$\left[\tilde{A}^{(3)} \right]_{\ell y} = \frac{C_A}{N_c} \gamma_0^2 G^{(3)}, \quad (33)$$

with

$$\left[\hat{A}^{(3)} \right]_{\ell y} = \left\{ \left[\left(C_{A_{123}}^{(3)} - 1 \right) - \left(C_{A_{12}}^{(2)} - 1 \right) - \left(C_{A_{13}}^{(2)} - 1 \right) - \left(C_{A_{23}}^{(2)} - 1 \right) \right] A_1 A_2 A_3 \right\}_{\ell y}, \quad (34)$$

after having set $A^{(3)} = C_{A_{123}}^{(3)} A_1 A_2 A_3$ for the three-particle correlator and $A_{ij}^{(2)} = C_{A_{ij}}^{(2)} A_i A_j$ for the two-particle correlator. We fix the anomalous dimension to the characteristic hardness of the jet $Q \approx E\Theta_0$

($\gamma_0^2(E\Theta_0) = \text{const}$) and solve this equation iteratively by derivating the r.h.s. of (34) with respect to ℓ and y , such that the solution of (33) reads

$$\begin{aligned} & \left(\dot{C}_{A_{123}}^{(3)} - 1 \right) - \left(\dot{C}_{A_{12}}^{(2)} - 1 \right) - \left(\dot{C}_{A_{13}}^{(2)} - 1 \right) - \left(\dot{C}_{A_{23}}^{(2)} - 1 \right) \\ &= \frac{N_c}{C_A} \frac{\left(\dot{C}_{A_{12}}^{(2)} - 1 \right) + \left(\dot{C}_{A_{13}}^{(2)} - 1 \right) + \left(\dot{C}_{A_{23}}^{(2)} - 1 \right)}{2 + \tilde{\Delta}_{12} + \tilde{\Delta}_{13} + \tilde{\Delta}_{23}} + \frac{N_c^2}{C_A^2} \frac{1}{2 + \tilde{\Delta}_{12} + \tilde{\Delta}_{13} + \tilde{\Delta}_{23}}, \end{aligned} \quad (35)$$

which have been written in terms of the logarithmic derivatives of the one-particle spectrum,

$$\tilde{\Delta}_{ij} = \gamma_0^{-2} (\psi_{A_i, \ell} \psi_{A_j, y} + \psi_{A_i, y} \psi_{A_j, \ell}), \quad \psi_{A_i, \ell} = \frac{1}{A_i} \frac{\partial A_i}{\partial \ell}, \quad \psi_{A_i, y} = \frac{1}{A_i} \frac{\partial A_i}{\partial y} \quad (36)$$

and the DLA two-particle correlator [6, 16] (for a review see also [28])

$$\dot{C}_{A_{ij}}^{(2)} - 1 = \frac{N_c}{C_A} \frac{1}{1 + \Delta_{ij}}. \quad (37)$$

The dot over $C^{(n)}$ differentiates the DLA correlators from the MLLA correlators obtained below. In DLA however, since the single inclusive distribution satisfies $Q = \frac{C_F}{N_c} G$ [27], one has

$$\psi_{Q_i, \ell} = \psi_{G_i, \ell} \equiv \psi_{i, \ell}, \quad \psi_{Q_i, y} = \psi_{G_i, y} \equiv \psi_{i, y}.$$

That is why, we will use the much simplest notation $\psi_{G_i, \ell} = \psi_{i, \ell}$, $\psi_{G_i, y} = \psi_{i, y}$. It is worth giving the order of magnitude of some quantities that will be considered in forthcoming calculations. In DLA, the one-particle inclusive distribution can be written as $A_i(\ell, y) \propto \exp(2\gamma_0 \sqrt{\ell y})$ asymptotically for fixed running coupling $\gamma_0 = \text{const}$ [27]. Though the solution with fixed coupling constant provides general features of the single inclusive distribution, it is not enough for the description of a more realistic picture at colliders. However, from its simplicity, it can be used to give the order of magnitude of terms involved in the solution of the DLA and MLLA evolution equations. Therefore, making use of (36), one has

$$\psi_{A_i, \ell} = \mathcal{O}(\gamma_0), \quad \psi_{A_i, y} = \mathcal{O}(\gamma_0), \quad \psi_{A_i, \ell \ell} = \mathcal{O}(\gamma_0^2), \quad \psi_{A_i, \ell y} = \mathcal{O}(\gamma_0^2), \quad \psi_{A_i, yy} = \mathcal{O}(\gamma_0^2), \quad (38)$$

$$\tilde{\Delta}_{ij} = \mathcal{O}(1), \quad \tilde{\Delta}_{ij, \ell} = \mathcal{O}(\gamma_0^2), \quad \tilde{\Delta}_{ij, y} = \mathcal{O}(\gamma_0^2), \quad (39)$$

where $\psi_{A_i, \ell \ell}$, $\psi_{A_i, \ell y}$ and $\psi_{A_i, yy}$ are double derivatives of $\psi_{A_i} = \ln A_i(\ell, y)$. The DLA solution (35) describes the following picture: the first term ($= -1$) in the l.h.s. translates the independent or decorrelated emission of three hadrons in the shower like depicted by Fig.2a. After inserting the two-particle correlator (37) in the l.h.s. of (35), terms $\propto \frac{N_c}{C_A}$ correspond to the case where two partons are correlated inside the same subjet, while the other one is emitted independently from the rest like in Fig.2b. Next, replacing (37) in the r.h.s. of (35) one obtains a contribution $\propto \frac{N_c^2}{C_A^2}$ described by Fig.2c, where two partons are emitted independently inside the same subjet. The last term $\propto \frac{N_c^2}{C_A^2}$ depicted by Fig.2d, involves three particles strongly correlated inside the same partonic shower and corresponds to the cumulant of genuine correlations. Actually, this interpretation has been given after computing the color factors of such Feynman diagrams describing the process, normalized by C_A^3 in the end. Notice that diagrams displayed in Fig.2c and Fig.2d present the same color factors but different Lorentz structure. In both cases, the DLA strong AO $\Theta \gg \Theta' \gg \Theta''$ and strong energy ordering $x_1 \gg x_2 \gg x_3$ are necessary conditions satisfied by (33) [29].

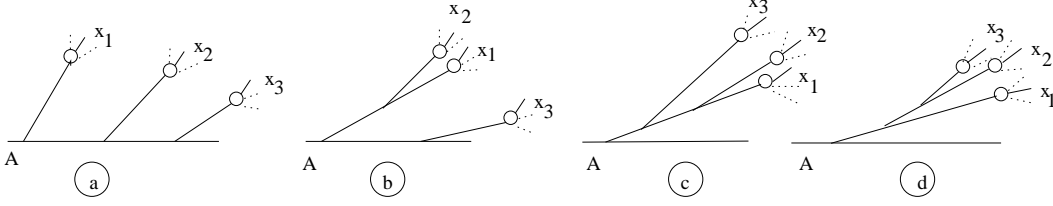


Figure 2: Three particles emitted inside the shower with color factors for the square of the amplitudes: C_A^3 , $C_A^2 N_c$, $C_A N_c^2$ and $C_A N_c^2$ for a, b, c and d respectively.

Performing the steepest descent evaluation of the DLA single inclusive distribution from an integral representation, which was written in Mellin space in the form [16, 27],

$$G(\ell, y) = (\ell + y + \lambda) \iint \frac{d\omega d\nu}{(2\pi i)^2} e^{\omega\ell + \nu y} \int_0^\infty \frac{ds}{\nu + s} \left(\frac{\omega(\nu + s)}{(\omega + s)\nu} \right)^{1/\beta_0(\omega - \nu)} e^{-\lambda s}, \quad Q = \frac{C_F}{N_c} G. \quad (40)$$

and which accounts for the running of the coupling α_s , the energy of most particles inside the jet was proved to be close to the maximum of the distribution, which shapes like a Gaussian in this region [27],

$$A_i(\ell_i, Y) \simeq \exp \left[-\frac{3}{\sqrt{\beta_0}} \frac{(\ell_i - \ell_{max})^2}{Y^{3/2}} \right], \quad \ell_{max} \approx \frac{Y}{2}. \quad (41)$$

From this method [16], the expressions of the logarithmic derivative of the one particle distribution were written as,

$$\psi_{i,\ell}(\mu_i, \nu_i) = \gamma_0 e^{\mu_i}, \quad \psi_{i,y}(\mu, \nu) = \gamma_0 e^{-\mu_i}. \quad (42)$$

such that Δ_{ij} and the correlator were given in the form [16],

$$\Delta_{ij} = 2 \cosh(\mu_i - \mu_j), \quad \dot{C}_{A_{ij}}^{(2)} = 1 + \frac{N_c}{C_A} \frac{1}{1 + 2 \cosh(\mu_i - \mu_j)} \quad (43)$$

respectively, where (μ_i, ν_i) were related to (ℓ_i, y_i) through the 2x2 non-linear system of equations [16],

$$\frac{y_i - \ell_i}{y_i + \ell_i} = \frac{(\sinh 2\mu_i - 2\nu_i) - (\sinh 2\nu_i - 2\mu_i)}{2(\sinh^2 \mu_i - \sinh^2 \nu_i)}, \quad \frac{\sinh \nu_i}{\sqrt{\lambda}} = \frac{\sinh \mu_i}{\sqrt{\ell_i + y_i + \lambda}}. \quad (44)$$

Therefore, the DLA three-particle correlator reads in this approximation

$$\begin{aligned} \dot{C}_{A_{123}}^{(3)} &= 1 + \left(\dot{C}_{A_{12}}^{(2)} - 1 \right) + \left(\dot{C}_{A_{13}}^{(2)} - 1 \right) + \left(\dot{C}_{A_{23}}^{(2)} - 1 \right) \\ &+ \frac{N_c}{2C_A} \frac{\left(\dot{C}_{A_{12}}^{(2)} - 1 \right) + \left(\dot{C}_{A_{13}}^{(2)} - 1 \right) + \left(\dot{C}_{A_{23}}^{(2)} - 1 \right)}{1 + \cosh(\mu_1 - \mu_2) + \cosh(\mu_1 - \mu_3) + \cosh(\mu_2 - \mu_3)} \\ &+ \frac{N_c^2}{2C_A^2} \frac{1}{1 + \cosh(\mu_1 - \mu_2) + \cosh(\mu_1 - \mu_3) + \cosh(\mu_2 - \mu_3)}. \end{aligned} \quad (45)$$

with $\dot{C}_{A_{ij}}^{(2)}$ extracted from (43). Taking $|\ell_i - \ell_{max}| \ll \sigma \propto Y^{3/2}$ for $i = 1, 2, 3$, one has in this approximation (see appendix C.2)

$$\Delta_{ij} \approx 2 + 9 \left(\frac{\ell_i - \ell_j}{Y} \right)^2 = 2 + 9 \left[\frac{\ln(x_j/x_i)}{\ln(Q/Q_0)} \right]^2, \quad (46)$$

so that,

$$\begin{aligned}\Delta_{12} + \Delta_{13} + \Delta_{23} &\approx 6 + 9 \left(\frac{\ell_1 - \ell_2}{Y} \right)^2 + 9 \left(\frac{\ell_1 - \ell_3}{Y} \right)^2 + 9 \left(\frac{\ell_2 - \ell_3}{Y} \right)^2 \\ &= 6 + 9 \left[\frac{\ln(x_2/x_1)}{\ln(Q/Q_0)} \right]^2 + 9 \left[\frac{\ln(x_3/x_1)}{\ln(Q/Q_0)} \right]^2 + 9 \left[\frac{\ln(x_3/x_2)}{\ln(Q/Q_0)} \right]^2.\end{aligned}\quad (47)$$

Therefore, the shape of the three-particle correlator can be expected to be quadratic as a function of the difference $(\ell_i - \ell_j)$, as for the two-particle correlator. Thus, the correlator is strongest when particles have the same energy $x_1 = x_2 = x_3$.

Moreover, the decreasing behavior of the correlator as one parton gets much harder than the others $x_i \gg x_j$ shows that QCD coherence effects dominate this region of the phase space as interferences between such gluons occur. New kinds of contributions like the one in the first term of the r.h.s. of (35) appear in this context.

The overall normalization of the n -particle correlator is fixed by that of the same rank multiplicity-correlator determining the multiplicity fluctuations inside the jet [16],

$$C_A^{(k)}(x_1, \dots, x_k) \leq \frac{\langle n(n-1) \dots (n-k+1) \rangle}{\langle n \rangle^k}.$$

Then, one has

$$C_A^{(2)}(x_1, x_2) - 1 \leq \frac{N_c}{3C_A}, \quad C_A^{(3)}(x_1, x_2, x_3) - 1 \leq \frac{N_c}{C_A} + \frac{N_c^2}{4C_A^2}. \quad (48)$$

These bounds can also be obtained by setting $\Delta(x_i, x_j) = 2$ (for $x_i = x_j$) in (37) and (35) respectively. Since DLA neglects the energy balance, it is not realistic and does not provide the real physical picture of any jet process in the frame of jet calculus.

2.5 Iterative solution of the evolution equations

As we can see, the computation of three-particle correlations requires a mastering knowledge of the one-particle inclusive energy distribution and two-particle correlations. The behavior of the two-particle correlators as shown by these solutions was proved to be quadratic as a function of $(\ell_i - \ell_j)$ and increasing as a function of $(\ell_i + \ell_j)$ like in the Fong-Webber approximation [17, 18]. However, the solutions (92, 93) (see appendix A.1) were shown to better account for soft gluon coherence effects, by describing the flattening of the slopes as $(\ell_i + \ell_j)$ increases. In [25], the solution was obtained by the steepest descent evaluation of the spectrum $G_i(\ell, y)$, while in [19], the evaluation was performed by taking the expression of $G_i(\ell, y)$ given by (89) in the appendix A.1. In [19], the solution of the evolution equations for two-particle correlation were obtained from the differential version of the equations (90, 91) over ℓ and y written in the appendix A.1. Therefore, in this subsection, we will make some transformations in order to simplify this cumbersome task without adding further information. In the appendix A.1, we briefly summarize what should be known in order to complete the solution of the evolution equations for the three-particle correlations.

Differentiating (28) and (29) with respect to “ ℓ ”, one has the differential system of evolution equations

for three-particle correlations,

$$\hat{Q}_{\ell y}^{(3)} = \frac{C_F}{N_c} \gamma_0^2 G^{(3)} - \frac{3}{4} \frac{C_F}{N_c} \gamma_0^2 \left(G_\ell^{(3)} - \beta_0 \gamma_0^2 G^{(3)} \right), \quad (49)$$

$$\begin{aligned} \hat{G}_{\ell y}^{(3)} = & \gamma_0^2 G^{(3)} - a \gamma_0^2 \left(G_\ell^{(3)} - \beta_0 \gamma_0^2 G^{(3)} \right) + (a-b) \gamma_0^2 \left\{ \left[\left(G_{12}^{(2)} - G_1 G_2 \right) G_3 \right. \right. \\ & + \left. \left(G_{13}^{(2)} - G_1 G_3 \right) G_2 + \left. \left(G_{23}^{(2)} - G_2 G_3 \right) G_1 \right]_\ell - \beta_0 \gamma_0^2 \left[\left(G_{12}^{(2)} - G_1 G_2 \right) G_3 \right. \right. \\ & + \left. \left(G_{13}^{(2)} - G_1 G_3 \right) G_2 + \left. \left(G_{23}^{(2)} - G_2 G_3 \right) G_1 \right] \right\} + (a-c) \gamma_0^2 \left[(G_1 G_2 G_3)_\ell - \beta_0 \gamma_0^2 G_1 G_2 G_3 \right], \end{aligned} \quad (50)$$

which is written in this paper for the first time. The equation (50) is self-contained and can be solved iteratively like (33). For this purpose, one sets $G^{(3)} = C_{G_{123}}^{(3)} G_1 G_2 G_3$ and $G_{ij}^{(2)} = C_{G_{ij}}^{(2)} G_i G_j$ in the left and right hand sides of (50), such that the solution obtained in the appendix B can be written in the compact form

$$C_{G_{123}}^{(3)} - 1 = \left(C_{G_{12}}^{(2)} - 1 \right) F_{12}^{(2)} + \left(C_{G_{13}}^{(2)} - 1 \right) F_{13}^{(2)} + \left(C_{G_{23}}^{(2)} - 1 \right) F_{23}^{(2)} + F_{123}^{(3)}, \quad (51)$$

where,

$$F_{ij}^{(2)} = 1 + \frac{N_{G_{ij}}^{(2)}}{D_G^{(2)}}, \quad F_{123}^{(3)} = \frac{N_G^{(3)}}{D_G^{(3)}}, \quad (52)$$

with

$$N_{G_{ij}}^{(2)} = 1 - b \left(\psi_{1,\ell} + \psi_{2,\ell} + \psi_{3,\ell} - \beta_0 \gamma_0^2 \right) - a \zeta_\ell + (a-b) \chi_\ell^{ij} + \xi_1^{ij} + \delta_2^{ij} - \epsilon_1 - \epsilon_2, \quad (53a)$$

$$D_G^{(2)} = 2 + \Delta_{12} + \Delta_{13} + \Delta_{23} + a \zeta_\ell + 2a \beta_0 \gamma_0^2 + \epsilon_1 + \epsilon_2, \quad (53b)$$

$$\begin{aligned} N_G^{(3)} = & 1 - c \left(\psi_{1,\ell} + \psi_{2,\ell} + \psi_{3,\ell} - \beta_0 \gamma_0^2 \right) - a \zeta_\ell + (a-b) (\chi_\ell^{12} + \chi_\ell^{13} + \chi_\ell^{23}) + (\xi_1^{12} + \delta_2^{12}) \\ & + (\xi_1^{13} + \delta_2^{13}) + (\xi_1^{23} + \delta_2^{23}) - \epsilon_1 - \epsilon_2, \end{aligned} \quad (53c)$$

$$D_G^{(3)} = D_G^{(2)} = 2 + \Delta_{12} + \Delta_{13} + \Delta_{23} + a \zeta_\ell + 2a \beta_0 \gamma_0^2 + \epsilon_1 + \epsilon_2. \quad (53d)$$

The solution (51) can be checked to recover the DLA result (35) inside a gluon jet, that is for $C_A = N_c$. Since DLA neglects recoil effects at each splitting inside the cascade, one should expect the DLA three-particle correlation to be much larger than MLLA predictions and therefore to overestimate the data. We introduce the following notations and give the order of magnitude of each contribution following from (38) and (39),

$$\zeta = \ln \dot{C}_{G_{123}}^{(3)}, \quad \zeta_\ell = \frac{\dot{C}_{G_{123},\ell}^{(3)}}{\dot{C}_{G_{123}}^{(3)}} = \mathcal{O}(\gamma_0^2), \quad \zeta_y = \frac{\dot{C}_{G_{123},y}^{(3)}}{\dot{C}_{G_{123}}^{(3)}} = \mathcal{O}(\gamma_0^2), \quad (54a)$$

$$\chi_\ell^{ij} = \frac{\dot{C}_{G_{ij},\ell}^{(2)}}{\dot{C}_{G_{ij}}^{(2)}} = \mathcal{O}(\gamma_0^2), \quad \chi_y^{ij} = \frac{\dot{C}_{G_{ij},y}^{(2)}}{\dot{C}_{G_{ij}}^{(2)}} = \mathcal{O}(\gamma_0^2), \quad (54b)$$

$$\xi_1^{ij} = \frac{1}{\gamma_0^2} \left[\chi_\ell^{ij} (\psi_{1,y} + \psi_{2,y} + \psi_{3,y}) + \chi_y^{ij} (\psi_{1,\ell} + \psi_{2,\ell} + \psi_{3,\ell}) \right] = \mathcal{O}(\gamma_0), \quad (54c)$$

$$\delta_2^{ij} = \frac{1}{\gamma_0^2} \left(\chi_\ell^{ij} \chi_y^{ij} + \chi_{\ell,y}^{ij} \right) = \mathcal{O}(\gamma_0^2), \quad (54d)$$

$$\epsilon_1 = \frac{1}{\gamma_0^2} \left[\zeta_\ell (\psi_{1,y} + \psi_{2,y} + \psi_{3,y}) + \zeta_y (\psi_{1,\ell} + \psi_{2,\ell} + \psi_{3,\ell}) \right] = \mathcal{O}(\gamma_0), \quad (54e)$$

$$\epsilon_2 = \frac{1}{\gamma_0^2} (\zeta_\ell \zeta_y + \zeta_{\ell,y}) = \mathcal{O}(\gamma_0^2). \quad (54f)$$

The solution of the gluon evolution equation for the correlator can be either obtained numerically by solving (50) or by performing the evaluation from the previous solution (51). However, in this paper, we will directly compute the solution (51) from the steepest descent method introduced in [25] and make some approximations in subsection 2.6. Accordingly, the solution of (49) is also obtained in the appendix B by setting $Q^{(3)} = C_{Q_{123}}^{(3)} Q_1 Q_2 Q_3$ and $Q_{ij}^{(2)} = C_{Q_{ij}}^{(2)} Q_i Q_j$ in the l.h.s. of (49) and $G^{(3)} = C_{G_{123}}^{(3)} G_1 G_2 G_3$ in the r.h.s. of the same equation, such that,

$$C_{Q_{123}}^{(3)} - 1 = \left(C_{Q_{12}}^{(2)} - 1\right) \tilde{F}_{12}^{(2)} + \left(C_{Q_{13}}^{(2)} - 1\right) \tilde{F}_{13}^{(2)} + \left(C_{Q_{23}}^{(2)} - 1\right) \tilde{F}_{23}^{(2)} + \tilde{F}_{123}^{(3)}, \quad (55)$$

where,

$$\tilde{F}_{ij}^{(2)} = 1 + \frac{N_{Q_{ij}}^{(2)}}{D_Q^{(2)}}, \quad \tilde{F}_{123}^{(3)} = \frac{N_Q^{(3)}}{D_Q^{(3)}}, \quad (56)$$

with

$$N_{Q_{ij}}^{(2)} = \tilde{\xi}_1^{ij} + \tilde{\delta}_2^{ij} - \tilde{\epsilon}_1 - \tilde{\epsilon}_2, \quad (57a)$$

$$D_Q^{(2)} = \tilde{\Delta}_{12} + \tilde{\Delta}_{13} + \tilde{\Delta}_{23} + \sum_i \frac{Q_{i\ell y}}{\gamma_0^2 Q_i} + \tilde{\epsilon}_1 + \tilde{\epsilon}_2, \quad (57b)$$

$$N_Q^{(3)} = \frac{C_F}{N_c} C_{G_{123}}^{(3)} \left[1 - \frac{3}{4} (\psi_{1,\ell} + \psi_{2,\ell} + \psi_{3,\ell} + \zeta_\ell - \beta_0 \gamma_0^2) \right] \frac{G_1 G_2 G_3}{Q_1 Q_2 Q_3} + (\tilde{\xi}_1^{12} + \tilde{\delta}_2^{12}) \quad (57c)$$

$$+ (\tilde{\xi}_1^{13} + \tilde{\delta}_2^{13}) + (\tilde{\xi}_1^{23} + \tilde{\delta}_2^{23}) - \tilde{\epsilon}_1 - \tilde{\epsilon}_2, \quad (57d)$$

$$D_Q^{(3)} = D_Q^{(2)} = \tilde{\Delta}_{12} + \tilde{\Delta}_{13} + \tilde{\Delta}_{23} + \sum_i \frac{Q_{i\ell y}}{\gamma_0^2 Q_i} + \tilde{\epsilon}_1 + \tilde{\epsilon}_2,$$

where one find the list of corrections,

$$\tilde{\zeta} = \ln \dot{C}_{Q_{123}}^{(3)}, \quad \tilde{\zeta}_\ell = \frac{\dot{C}_{Q_{123},\ell}^{(3)}}{\dot{C}_{Q_{123}}^{(3)}} = \mathcal{O}(\gamma_0^2), \quad \tilde{\zeta}_y = \frac{\dot{C}_{Q_{123},y}^{(3)}}{\dot{C}_{Q_{123}}^{(3)}} = \mathcal{O}(\gamma_0^2), \quad (58a)$$

$$\tilde{\chi}_\ell^{ij} = \frac{\dot{C}_{Q_{ij},\ell}^{(2)}}{\dot{C}_{Q_{ij}}^{(2)}} = \mathcal{O}(\gamma_0^2), \quad \tilde{\chi}_y^{ij} = \frac{\dot{C}_{Q_{ij},y}^{(2)}}{\dot{C}_{Q_{ij}}^{(2)}} = \mathcal{O}(\gamma_0^2), \quad (58b)$$

$$\tilde{\xi}_1^{ij} = \frac{1}{\gamma_0^2} \left[\tilde{\chi}_\ell^{ij} (\psi_{Q_1,y} + \psi_{Q_2,y} + \psi_{Q_3,y}) + \tilde{\chi}_y^{ij} (\psi_{Q_1,\ell} + \psi_{Q_2,\ell} + \psi_{Q_3,\ell}) \right] = \mathcal{O}(\gamma_0), \quad (58c)$$

$$\tilde{\delta}_2^{ij} = \frac{1}{\gamma_0^2} \left(\tilde{\chi}_\ell^{ij} \tilde{\chi}_y^{ij} + \tilde{\chi}_{\ell,y}^{ij} \right) = \mathcal{O}(\gamma_0^2), \quad (58d)$$

$$\tilde{\epsilon}_1 = \frac{1}{\gamma_0^2} \left[\tilde{\zeta}_\ell (\psi_{Q_1,y} + \psi_{Q_2,y} + \psi_{Q_3,y}) + \tilde{\zeta}_y (\psi_{Q_1,\ell} + \psi_{Q_2,\ell} + \psi_{Q_3,\ell}) \right] = \mathcal{O}(\gamma_0), \quad (58e)$$

$$\tilde{\epsilon}_2 = \frac{1}{\gamma_0^2} \left(\tilde{\zeta}_\ell \tilde{\zeta}_y + \tilde{\zeta}_{\ell,y} \right) = \mathcal{O}(\gamma_0^2). \quad (58f)$$

The order of magnitude of these terms follows from (38) and (39). Setting all corrections to zero, one recovers the DLA solution (35) for $C_A = C_F$. The solutions (51) and (55) of the evolution equations entangle corrections of order $\mathcal{O}(\gamma_0)$ and $\mathcal{O}(\gamma_0^2)$, which are MLLA and NMLLA respectively. Furthermore, every term in (51) and (55) can be associated to a Feynman diagram of Fig.2 as was explained in subsection 2.4. The functions $F_{123}^{(3)}$ and $\tilde{F}_{123}^{(3)}$ in (51) and (55) correspond respectively to the cumulant of genuine correlations associated to the process displayed in Fig.1 and Fig.2d. These contributions, (54a-54f) and (58a-58f) are small corrections arising from the iterative solution of the evolution equations because one

takes the derivatives over the functions $\zeta = \ln \dot{C}_{G_{123}}^{(3)}$, $\tilde{\zeta} = \ln \dot{C}_{Q_{123}}^{(3)}$ and $\chi^{ij} = \ln \dot{C}_{G_{ij}}^{(2)}$, $\tilde{\chi}^{ij} = \ln \dot{C}_{Q_{ij}}^{(2)}$ for both quark and gluon jets. For the evaluation of such corrections one needs to take the DLA expressions of $\dot{C}_{A_{123}}^{(3)}$ and $\dot{C}_{A_{ij}}^{(2)}$ written in (35) and (37) respectively.

2.6 MLLA approximation and evaluation by the steepest descent method

In [19], the exact solutions of the two-particle evolution equations were compared with the MLLA solutions from the steepest descent method for the one particle distribution. The agreement between both approaches was successful and made possible the fast computation of the correlators from the steepest descent. That is the reason for in this paper, we limit ourselves to this method. Making use of the ratio (87), it is easy to demonstrate that,

$$\psi_{Q,\ell} = \psi_\ell + \mathcal{O}(\gamma_0^2), \quad \psi_{Q,y} = \psi_y + \mathcal{O}(\gamma_0^2), \quad \tilde{\Delta}_{ij}^{mla} = \Delta_{ij} + \mathcal{O}(\gamma_0^2). \quad (59)$$

Dropping corrections of order $\mathcal{O}(\gamma_0^2)$, which go beyond the MLLA approximation, we obtain for the gluon jet

$$F_{ij}^{(2)} \stackrel{mla}{=} 1 + \frac{1 - b(\psi_{1,\ell} + \psi_{2,\ell} + \psi_{3,\ell}) + \xi_1^{ij} - \epsilon_1}{2 + \Delta_{12} + \Delta_{13} + \Delta_{23} + \epsilon_1}, \quad (60)$$

$$F_{123}^{(3)} \stackrel{mla}{=} \frac{1 - c(\psi_{1,\ell} + \psi_{2,\ell} + \psi_{3,\ell}) + \xi_1^{12} + \xi_1^{13} + \xi_1^{23} - \epsilon_1}{2 + \Delta_{12} + \Delta_{13} + \Delta_{23} + \epsilon_1} \quad (61)$$

and for the quark jet

$$\tilde{F}_{ij}^{(2)} \stackrel{mla}{=} 1 + \frac{\tilde{\xi}_1^{ij} - \tilde{\epsilon}_1}{3 + \Delta_{12} + \Delta_{13} + \Delta_{23} - a(\psi_{1,\ell} + \psi_{2,\ell} + \psi_{3,\ell}) + \tilde{\epsilon}_1}, \quad (62)$$

$$\tilde{F}_{123}^{(3)} \stackrel{mla}{=} \frac{N_c^2 \mathcal{C}_{G_{123}}^{(3)} [1 - a(\psi_{1,\ell} + \psi_{2,\ell} + \psi_{3,\ell})] + \tilde{\xi}_1^{12} + \tilde{\xi}_1^{13} + \tilde{\xi}_1^{23} - \tilde{\epsilon}_1}{C_F^2 [3 + \Delta_{12} + \Delta_{13} + \Delta_{23} - a(\psi_{1,\ell} + \psi_{2,\ell} + \psi_{3,\ell}) + \tilde{\epsilon}_1]}. \quad (63)$$

The subtracted terms $\propto -a$ in the denominators of (62) and (63) appear after having replaced (87) and (88) in (57b) and (57c) respectively. Such simplified expressions are useful for the steepest descent evaluation that proved successful while describing the single inclusive distribution and two-particle correlations in [25]. Except the MLLA corrections ϵ_1 and ξ_1^{ij} , all the other corrections and functions appearing in the solutions of the evolution equations were obtained in [25], which will allow for the straightforward computation of the three-particle correlators in quark and gluon jets. We write some of these formulæ for the evaluation in the appendix C. Integrating the equation (81) over “ y ”, the solution for the single inclusive distribution is given by the following integral representation in Mellin space [25],

$$G(\ell, y) = (\ell + y + \lambda) \iint \frac{d\omega d\nu}{(2\pi i)^2} e^{\omega\ell + \nu y} \int_0^\infty \frac{ds}{\nu + s} \left(\frac{\omega(\nu + s)}{(\omega + s)\nu} \right)^{1/\beta_0(\omega - \nu)} \left(\frac{\nu}{\nu + s} \right)^{a/\beta_0} e^{-\lambda s}. \quad (64)$$

The integral representation (64) was estimated by the steepest descent method at small $x \ll 1$ and high energy scale $Q \gg 1$; the approached solution was compared with the exact solution (89) (see the appendix A.1) in the limiting spectrum ($\lambda = 0$) and beyond ($\lambda \neq 0$). In particular, (64) was also demonstrated to be equivalent to (89) for $\lambda = 0$ [19]. The agreement between the approached and exact solutions turned out to be good, such that the following expressions of the approached logarithmic

derivatives from the steepest descent method were suited for the evaluation of the two-particle correlators [25],

$$\psi_{i,\ell}(\mu_i, \nu_i) = \gamma_0 e^{\mu_i} + \frac{1}{2} a \gamma_0^2 \left[e^{\mu_i} \tilde{Q}(\mu_i, \nu_i) - \tanh \nu_i - \tanh \nu_i \coth \mu_i \left(1 + e^{\mu_i} \tilde{Q}(\mu_i, \nu_i) \right) \right] \quad (65)$$

$$\begin{aligned} & - \frac{1}{2} \beta_0 \gamma_0^2 \left[1 + \tanh \nu_i \left(1 + K(\mu_i, \nu_i) \right) + C(\mu_i, \nu_i) \left(1 + e^{\mu_i} \tilde{Q}(\mu_i, \nu_i) \right) \right] + \mathcal{O}(\gamma_0^2), \\ \psi_{i,y}(\mu, \nu) &= \gamma_0 e^{-\mu_i} - \frac{1}{2} a \gamma_0^2 \left[2 + e^{-\mu_i} \tilde{Q}(\mu_i, \nu_i) + \tanh \nu_i - \tanh \nu_i \coth \mu_i \left(1 + e^{-\mu_i} \tilde{Q}(\mu_i, \nu_i) \right) \right] \\ & - \frac{1}{2} \beta_0 \gamma_0^2 \left[1 + \tanh \nu_i \left(1 + K(\mu_i, \nu_i) \right) - C(\mu_i, \nu_i) \left(1 + e^{-\mu_i} \tilde{Q}(\mu_i, \nu_i) \right) \right] + \mathcal{O}(\gamma_0^2), \end{aligned} \quad (66)$$

where the functions $\tilde{Q}(\mu_i, \nu_i)$, $C(\mu_i, \nu_i)$ and $K(\mu_i, \nu_i)$ are defined in the appendix C. The term $\propto a$ in (65) and (66) accounts for energy conservation while that $\propto \beta_0$ accounts for the running of the coupling α_s . The variables (μ_i, ν_i) are related to (ℓ_i, y_i) through the same 2x2 non-linear system of equations (44). After inverting (44) numerically, $\mu_i(\ell_i, y_i)$ and $\nu_i(\ell_i, y_i)$ can be plugged into (65) and (66) so as to get the logarithmic derivatives of the single inclusive spectrum as a function of the original kinematical variables ℓ_i and y_i as it was done in [25]. The MLLA two-particle correlators involved in (51) and (55) are (108) and (109) and are written in the appendix C. These expressions have been taken from reference [25].

Corrections $\xi_1^{ij}, \tilde{\xi}_1^{ij}$ and $\epsilon_1, \tilde{\epsilon}_1$ are new for three-particle correlations. Such expressions are explicitly written in the appendix C.1 from the steepest descent evaluation of the single inclusive distribution (64). They are small and decrease the three-particle correlator for $\ell_i \neq \ell_j$, that is when one parton is much harder than the other. Notice that the steepest descent method constitutes the only way for the disentanglement between MLLA $\mathcal{O}(\sqrt{\alpha_s})$ and NMLLA $\mathcal{O}(\alpha_s)$ corrections appearing in the solution of the evolution equations for the two and three-particle correlations. It makes also possible to distinguish between corrections following from the energy balance and the running effects of the coupling constant α_s . Finally, this method also allows for the application of the hump approximation or Fong-Webber expansion of the solutions with MLLA $\mathcal{O}(\sqrt{\alpha_s})$ accuracy [17, 18].

In this frame, the role of MLLA corrections should be expected to be larger than for the two-particle correlations. Indeed, higher order corrections increase with the rank of the correlator, which is known from the Koba-Nielsen-Olesen (KNO) problem for intra-jet multiplicity fluctuations [28, 30, 31]. For the 2-particle for instance one has $\propto -b(\psi_{1,\ell} + \psi_{2,\ell})$ and for the three-particle correlator one gets the larger correction $\propto -c(\psi_{1,\ell} + \psi_{2,\ell} + \psi_{3,\ell})$.

2.7 Hump approximation

From the steepest descent evaluation introduced in [25], near the hump of the single inclusive distribution $|\ell - Y/2| \ll \sigma \propto Y^{3/2}$ for $i = 1, 2, 3$, corrections $\xi_1^{ij}, \tilde{\xi}_1^{ij}$ and $\epsilon_1, \tilde{\epsilon}_1$ could be written in the symbolic form (see appendix C.2),

$$\xi_1^{ij}, \tilde{\xi}_1^{ij} \simeq \left(\frac{\ell_i - \ell_j}{Y} \right)^2 \gamma_0 + \mathcal{O}(\gamma_0^2), \quad (67)$$

$$\epsilon_1, \tilde{\epsilon}_1 \simeq \left(\frac{\ell_1 - \ell_2}{Y} \right)^2 \gamma_0 + \left(\frac{\ell_1 - \ell_3}{Y} \right)^2 \gamma_0 + \left(\frac{\ell_2 - \ell_3}{Y} \right)^2 \gamma_0 + \mathcal{O}(\gamma_0^2), \quad (68)$$

such that both can be neglected $\xi_1^{ij} \approx 0$, $\epsilon_1 \approx 0$ in this approximation, like δ_1^{ij} was also in [25]. In the appendix C.2, following from the steepest descent method, the expressions of (53a-53d) are given and

(57a-57d) expanded in $\sqrt{\alpha_s}$. In particular, the expressions (128e) and (128g), after being expanded in γ_0 , can be demonstrated to recover the Fong-Webber results for the two-particle correlations [17, 18]. Replacing the expressions (128a-128j) into (51,52) and (55,56), one finds those for the three-particle correlators in the Fong-Webber approximation [17, 18]. This solution will be compared with that from (61) and (63) after making use of (65) and (66) in subsection 3.

2.8 From two to three-particle correlations in the small x region

In [19], the sign of the two-particle correlator ($C_A^{(2)} - 1 \geq 0$) was studied as a function of x in the region of the phase space where the two partons (hadrons after assuming the LPHD) are strongly correlated. From the previous inequality, it turned out that two partons with $\ell_i \gtrsim 2.6$ ($x_i \lesssim 0.07$) at LHC energy scales (i.e. $Q = 450$ GeV, see subsection 3) are correlated as they are emitted from the same cascade following the QCD AO. Asymptotically $Y \rightarrow \infty$, one has $\ell_i \gtrsim 4.5$ ($x_i \lesssim 0.011$).

For three-particle correlations we study the sign of the cumulant of the genuine correlator $F_{123}^{(3)} > 0$ and determine the approximate region in x where diagrams displayed in Fig.1 and Fig.2d become dominant. One has,

$$1 - c(\psi_{1,\ell} + \psi_{2,\ell} + \psi_{3,\ell}) + \xi_1^{12} + \xi_1^{13} + \xi_1^{23} - \epsilon_1 > 0.$$

However, corrections ξ_1^{ij} , ϵ_1 have been shown to be negligible and to vanish for particles having the same energy momentum. Thus, we rather study the sign of

$$1 - c(\psi_{1,\ell} + \psi_{2,\ell} + \psi_{3,\ell}) > 0.$$

Making use of $\psi_\ell = \gamma_0 \sqrt{\frac{y}{\ell}} = \gamma_0 \sqrt{\frac{Y-\ell}{\ell}}$ for the sake of simplicity, one has,

$$1 - 3c\gamma_0 \sqrt{\frac{Y-\ell}{\ell}} > 0 \Leftrightarrow \ell > \frac{M}{1 + \frac{M}{Y}}, \quad M = \frac{9c^2}{\beta_0} = 10.1.$$

Thus, for LHC energy $Y = 7.5$, the value of $\ell(x)$ where the cumulant becomes positive turns out to be $\ell \gtrsim 4.3$, which in x corresponds to $x \lesssim 0.014$. Asymptotically $Y \rightarrow \infty$, one has $\ell_i \gtrsim 10.1$ ($x_i \lesssim 4.1 \times 10^{-5}$). Therefore, there exists a range in x where the observable $C_{123}^{(3)}$ is dominated by the emission of two correlated partons emitted independently from the third one, that is $0.014 \lesssim x \lesssim 0.07$ for diagrams Fig.2b and Fig.2c; for $x \lesssim 0.014$, the process will be dominated by three particles emitted from the same partonic cascade following the QCD AO described in Fig.2d. Asymptotically $Y \rightarrow \infty$, one has $4.1 \times 10^{-5} \lesssim x \lesssim 0.011$ for diagrams Fig.2b and Fig.2c, and $x \lesssim 4.1 \times 10^{-5}$ for Fig.2d. These values will indeed justify our choices for the representation of the three-particle correlations as function of (x_1, x_2, x_3) in subsection 3.

2.9 Beyond three-particle correlations

It is worth reminding that the LPHD hypothesis has also been confronted to multi-particle factorial moments up to the 5th order in the experimental studies of ep and e^+e^- collisions at HERA [34] and LEP [35] respectively, where it was found that the LPHD hypothesis faces difficulties when it is applied to soft multi-particle fluctuations. In this work the studies are carried out by using the momentum and transverse momentum cuts in order to test the MLLA soft limit calculations [33]. The theoretical computation of

multiplicity correlators or multiplicity fluctuations $\langle n(n-1)\dots(n-k+1) \rangle$ was performed in [32] at MLLA up to the rank $k = 5$ of the correlator.

However, performing these calculations for higher rank differential inclusive correlators, related to the previous ones by the integral

$$\langle n(n-1)\dots(n-k+1) \rangle_A = \int dx_1 \dots dx_k x_1 \dots x_k D_A^{(k)}(x_1, \dots, x_k, Y)$$

becomes rather cumbersome. As an example, in this subsection, we display the DLA equation and solution of the 4-particle correlator. The DLA equation reads,

$$\hat{A}_{1234}^{(4)} = \frac{C_A}{N_c} \gamma_0^2 G_{1234}^{(4)}, \quad (69)$$

where \hat{A} has been defined in the appendix D in (129). The solution of (69) with the definition of \hat{A} (129) reads,

$$C_A^{(4)} - 1 = \frac{N_c}{C_A} H_1(\dot{c}^{(2)}) + \frac{N_c^2}{C_A^2} H_2(\dot{c}^{(3)}, \dot{c}^{(2)}) + \frac{N_c^3}{C_A^3} \frac{H_3(\dot{c}^{(3)}, \dot{c}^{(2)})}{3 + \Delta_{12} + \Delta_{13} + \Delta_{14} + \Delta_{23} + \Delta_{24} + \Delta_{34}}, \quad (70)$$

where the functions H_1 , H_2 and H_3 are written in the appendix D in (130), (131) and (132) respectively. The solution (70) can also be interpreted in terms of Feynman diagrams contributing to the emission of four hadrons inside the jet. Accordingly, the term $\propto \frac{N_c}{C_A}$ correspond to the case $A \rightarrow 12(34)$ where two offspring are correlated while the other two are emitted independently; as a consequence it depends only on the two-particle correlator. The second term $\propto \frac{N_c^2}{C_A^2}$ is associated to the cases $A \rightarrow (12)(34)$ and $A \rightarrow (123)4$, which translates into either emitting two sub-jets with two-particles correlated within each, or emitting three correlated partons like in Fig.1 with another independent emission. Finally, the term $\propto \frac{N_c^3}{C_A^3}$ after setting $H_3 = 1 + \dots$ corresponds to the full correlated emission of four offspring inside the same shower. The inclusion of SLs corrections to (70) would be cumbersome and stays beyond the scope of this paper. On the other hand, the computation of differential higher order rank (k) correlators at MLLA would imply the failure of the perturbative approach because of the increasing size of higher order corrections $\propto (\psi_{1,\ell} + \dots \psi_{k,\ell}) = \mathcal{O}(\sqrt{\alpha_s})$. Hence, for higher order k correlators, the small x range where MLLA predictions stay valid gets reduced even at high energy scales, such that (see subsection 2.8)

$$M_k = \frac{k^2 c_k}{\beta_0}, \quad \ell_k > \frac{M_k}{1 + \frac{M_k}{Y}}$$

with

$$c_k = \frac{1}{4N_c} \left[\frac{11}{3} N_c + (-1)^k \frac{4}{3} n_f T_R \left(1 - 2 \frac{C_F}{N_c} \right)^k \right].$$

3 Predictions for the LHC and phenomenological consequences

In this section, we perform theoretical predictions for three-particle correlations for the LHC. We display the MLLA solutions (51) and (55) of the evolution equations (50) and (49) respectively. We compare the DLA solution of the evolutions equations from section 2.4 with the MLLA solution from the steepest descent evaluation of the one-particle distribution in subsection 2.6 and the solution from the hump approximation in 2.7. Thus,

- the DLA solution is computed by plugging (43) into (45);
- the MLLA solution from the steepest descent will be displayed by substituting the MLLA two-particle correlators (108), (109) and the functions (60), (61), (62) and (63) into (51) and (55) for gluon and quark jets respectively;
- the MLLA hump approximation will be displayed by plugging (128a)-(128j) into (52) and (56) and finally (51) and (55).

In particular, the computation of the DLA and MLLA solutions from the steepest descent needs the prior inversion of the system of equations (44) in order to obtain (μ_i, ν_i) as functions of the original kinematical variables (ℓ_i, y_i) . The correlators are functions of the variables (ℓ_i, y_i) and the virtuality of the jet $Q = E\Theta_0$. After setting $y_i = Y - \ell_i$ with fixed $Y = \ln(Q/Q_0)$ in the arguments of the solutions (51) and (55) the dependence can be reduced to the following: $\mathcal{C}_{G_{123}}^{(3)}(\ell_1, \ell_2, \ell_3, Y)$ and $\mathcal{C}_{Q_{123}}^{(3)}(\ell_1, \ell_2, \ell_3, Y)$.

3.1 Predictions for the limiting spectrum $\lambda \approx 0$

In this subsection we give predictions within the limiting spectrum $\lambda \lesssim 0.5$ for charged hadrons mostly composed by pions and kaons.

In Fig.3, the DLA (35), MLLA hump approximation from subsection 2.7 and MLLA (51) three-particle correlators are displayed, as a function of the difference $(\ell_1 - \ell_2) = \ln(x_2/x_1)$ for two fixed values of $\ell_3 = \ln(1/x_3) = 4.5, 5.5$, fixed sum $(\ell_1 + \ell_2) = |\ln(x_1 x_2)| = 10$ and finally fixed $Y = 7.5$ (virtuality $Q = 450$ GeV and $\Lambda_{QCD} = 250$ MeV), which is realistic for the LHC phenomenology [13]. The values $\ell_3 = \ln(1/x_3) = 4.5, 5.5$ ($x_3 = 0.011, x_3 = 0.004$) have been chosen according to the range of the energy fraction $x_i \ll 0.1$, where the MLLA scheme can only be applied and in particular, the range $x \lesssim 0.014$, where the cumulant correlator $F_{123}^{(3)}$ is dominant (see subsection 2.8).

In Fig.4, the DLA (35), MLLA hump approximation from subsection 2.7 and MLLA (51) three-particle correlators are displayed, in this case, as a function of the sum $(\ell_1 + \ell_2) = |\ln(x_1 x_2)|$ for the same values of $\ell_3 = \ln(1/x_3) = 4.5, 5.5$, for $x_1 = x_2$ and $Y = 7.5$. The range $7.0 \leq |\ln(x_1 x_2)| \leq 13.0$ has been chosen according to the condition $x \lesssim 0.014$ discussed in 2.8.

As expected in both cases, the DLA and MLLA three-particle correlators are larger inside a quark than in a gluon jet. Of course, these plots will be the same and the interpretation will apply to all possible permutations of three particles (123). As observed and written above, the difference between the DLA and MLLA results is quite important pointing out that overall corrections in $\mathcal{O}(\sqrt{\alpha_s})$ are quite large. Indeed, the last behavior is not surprising as was already observed on the treatment of multiplicity fluctuations of the third kind, where [32]

$$\frac{\langle n(n-1)(n-2) \rangle_G}{\langle n \rangle_G^3} = 2.25 [1 - (1.425 - 0.021n_f)\sqrt{\alpha_s}],$$

$$\frac{\langle n(n-1)(n-2) \rangle_Q}{\langle n \rangle_Q^3} = 4.52 [1 - (2.280 - 0.018n_f)\sqrt{\alpha_s}].$$

For instance, for one quark jet produced at the Z^0 peak of the e^+e^- annihilation ($Q = 45.6$ GeV), one has $\alpha_s = 0.134$. Replacing this value into the previous formula for a quark jet multiplicity correlator, one obtains a variation from 4.52 (DLA) to 0.83 (MLLA). That is one of the reasons for DLA has been

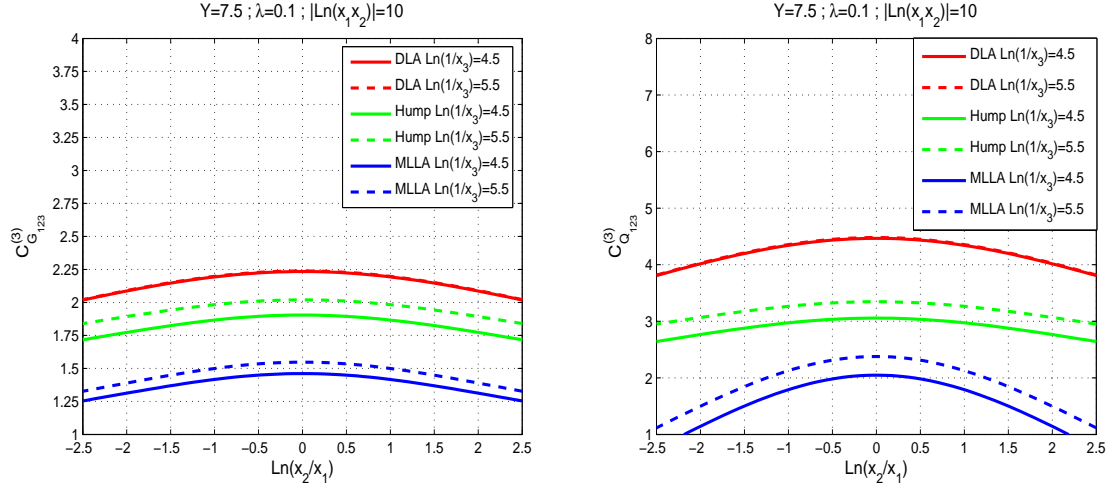


Figure 3: Three-particle correlations inside a gluon jet (left) and a quark jet (right) as a function of $\ell_1 - \ell_2 = \ln(x_2/x_1)$ for $\ell_1 + \ell_2 = |\ln(x_1 x_2)| = 10$, $\ell_3 = \ln(1/x_3) = 4.5, 5.5$, fixed $Y = 7.5$ in the limiting spectrum approximation $\lambda \approx 0$.

known to provide unreliable predictions which should not be compared with experiments. From Fig.3, the correlation are observed to be the strongest when particles have the same energy $x_i = x_j$ for fixed x_k and to decrease when one parton is much harder the others. Indeed, in this region of the phase space two competing effects should be satisfied: on one hand, as a consequence of gluon coherence and AO, gluon emission angles should decrease and on the other hand, the convergence of the perturbative series $k_\perp = x_i E \Theta_i \geq Q_0$ should be guaranteed. That is why, as the collinear cut-off parameter Q_0 is reached, gluons are emitted at larger angles and destructive interferences with previous emissions occur. Moreover, the observable increases for softer partons with x_3 decreasing, which is for partons less sensitive to the energy balance. In Fig.4 the MLLA correlations increase for softer partons, then flatten and decrease as a consequence of soft gluon coherence, reproducing for three-particle correlations, the hump-backed shape of the one-particle distribution. Because of the limitation of the phase space, one has $C^{(3)} \leq 1$ for harder partons. Finally, in Fig.5, we display the three-particle correlators as function of the sum $|\ln(x_1 x_2 x_3)|$, for $x_1 = x_2 = x_3$; when compared with Fig.4 and Fig.3, the correlators are shown to be larger. That is why, and as expected, the correlations are the strongest for particles having the same energy-momentum $x_1 = x_2 = x_3$. In these figures, the MLLA hump approximation is seen to become larger than the DLA correlator for smaller values of x than those close to the hump region, which is unphysical. This is due to the fact that this approximation should not be trusted beyond the hump region $|\ell - Y/2| \ll \sigma \propto Y^{3/2}$, $3Y/2 = 11.25$ in this case.

The MLLA hump approximation from subsection 2.7 is observed to be larger than the MLLA solution from the steepest descent of the one-particle distribution but one should bear in mind that this is only an approximation made for the sake of clarity in the interpretation of the solutions. In particular, from Fig.3 one can observe a smoother descent for the slope of the correlators in this case than that given from the more exact steepest descent. This difference comes from the role played by the iterative corrections displayed in Fig.8, which decrease the correlators away from the hump region when one of the partons becomes harder than the others. Near the maximum $x_i = x_j$ of the correlators, the difference between

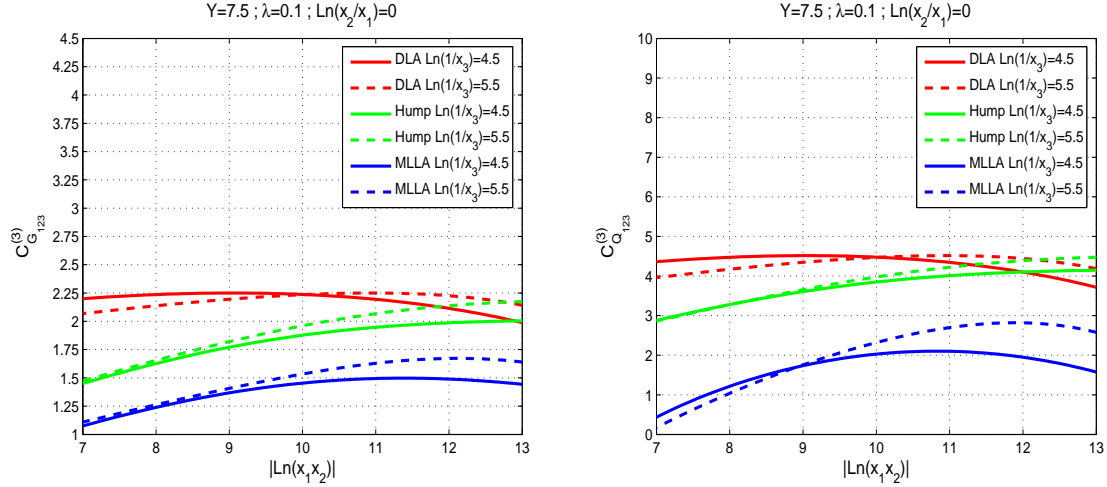


Figure 4: Three-particle correlations inside a gluon jet (left) and a quark jet (right) as a function of $\ell_1 + \ell_2 = |\ln(x_1 x_2)|$ for $x_1 = x_2$, $\ell_3 = \ln(1/x_3) = 4.5, 5.5$, fixed $Y = 7.5$ in the limiting spectrum approximation $\lambda \approx 0$.

the two approaches is $\mathcal{O}\left(\frac{\ell_k^2}{Y^2}\gamma_0\right)$ and should decrease for $x_i \rightarrow 1$, according to (68).

3.2 Predictions beyond the limiting spectrum $\lambda \neq 0$

The approximated evaluation of the one-particle distribution from the steepest descent method made possible the evaluation of the two-particle correlations beyond the limiting spectrum approximation, that is for $Q_0 \neq \Lambda_{QCD}$. Accordingly, it makes also possible the evaluation of the three-particle correlators $\mathcal{C}_{G_{123}}^{(3)}(\ell_1, \ell_2, \ell_3, Y)$ and $\mathcal{C}_{Q_{123}}^{(3)}(\ell_1, \ell_2, \ell_3, Y)$ beyond this limit $\lambda \neq 0$. This parameter, also known as hadronization parameter, guarantees in particular the convergence of the perturbative approach $\alpha_s \ll 1$. In Fig.6 and Fig.7 we display the same set of curves beyond the limiting spectrum ($\lambda = 1.5$) as in Fig.3 and Fig.4 in the limiting spectrum ($\lambda \sim 0$), with the exception of curves coming from the hump approximation. The value of λ in this case was evaluated for $Q_0 \sim 1$ GeV, which corresponds to the proton mass, and $\Lambda_{QCD} = 250$ MeV. As observed the correlation increases with λ and the range where $\mathcal{C}^{(3)} \geq 1$ becomes larger in this case.

4 Conclusions

In this paper we provide the first full pQCD treatment of three-particle correlations in parton showers and a further refined test of the LPHD within the limiting spectrum approximation and beyond. The evolution equations satisfied by this differential observable have been obtained for the first time and the differential version of the equations has been solved iteratively. It has been possible to interpret the analytical solution in terms of Feynman diagrams describing the process and to evaluate it from the steepest descent method applied to the single inclusive distribution. The correlations have been displayed in the range $x \lesssim 0.014$, where the process is dominated by three particles emitted from the same partonic cascade following the QCD AO described in Fig.1 and Fig.2d. Furthermore, four-particle correlations

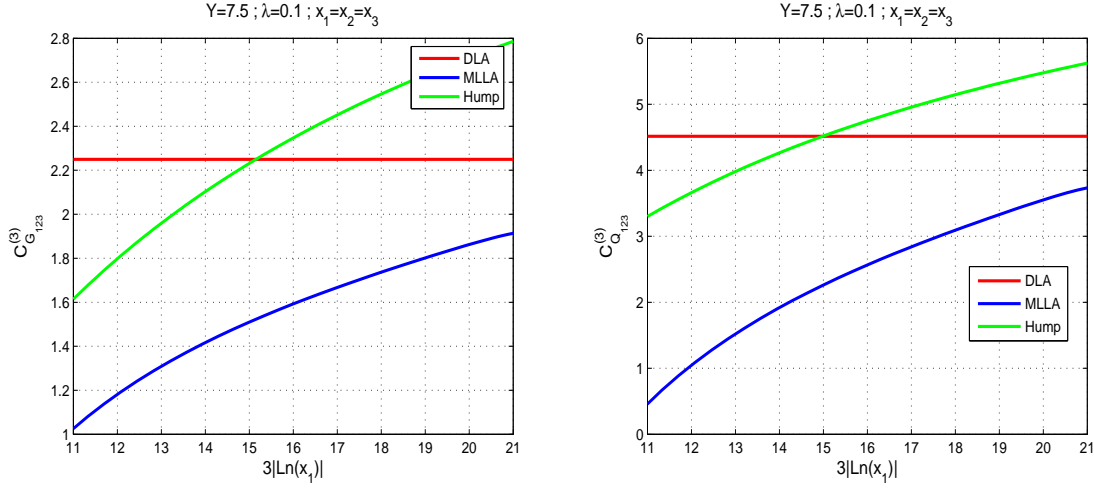


Figure 5: Three-particle correlations inside a gluon jet (left) and a quark jet (right) as a function of $\ell_1 + \ell_2 + \ell_3 = |\ln(x_1 x_2 x_3)|$ for $x_1 = x_2 = x_3$, fixed $Y = 7.5$ in the limiting spectrum approximation $\lambda \approx 0$.

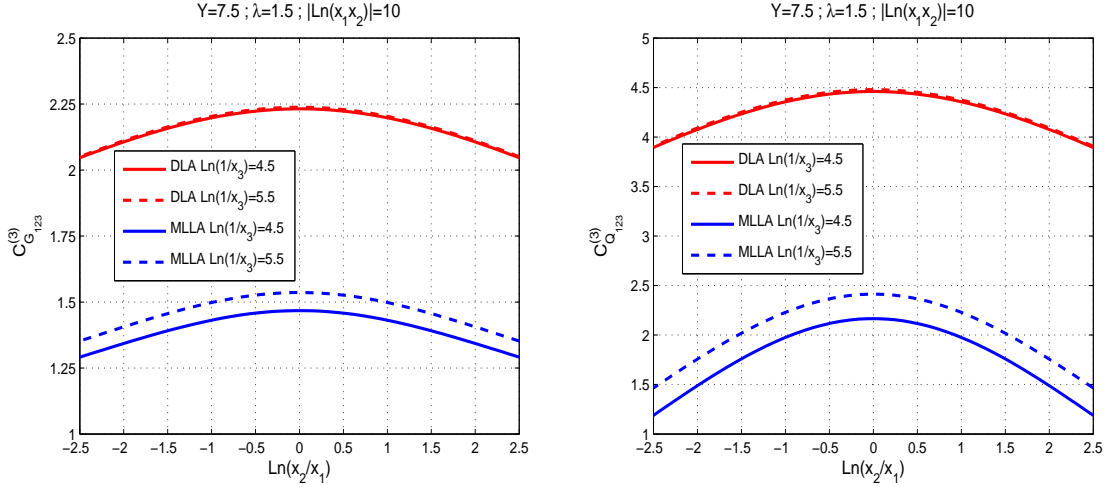


Figure 6: Three-particle correlations inside a gluon jet (left) and a quark jet (right) as a function of $\ell_1 - \ell_2 = \ln(x_2/x_1)$ for $\ell_1 + \ell_2 = |\ln(x_1 x_2)| = 10$, $\ell_3 = \ln(1/x_3) = 4.5, 5.5$, fixed $Y = 7.5$ in the limiting spectrum approximation $\lambda = 1.5$.

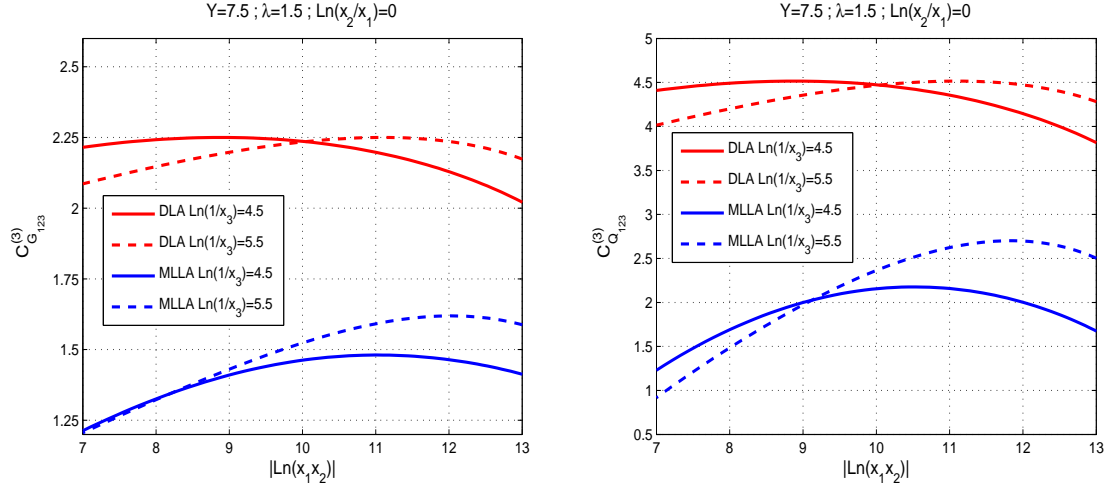


Figure 7: Three-particle correlations inside a gluon jet (left) and a quark jet (right) as a function of $\ell_1 + \ell_2 = |\ln(x_1 x_2)|$ for $x_1 = x_2$, $\ell_3 = \ln(1/x_3) = 4.5, 5.5$, fixed $Y = 7.5$ in the limiting spectrum approximation $\lambda = 1.5$.

have been computed at DLA so as to show that the inclusion of higher order corrections for more than three particles would rather be a cumbersome task. The correlations have been shown to be strongest for the softest hadrons having the same energy $x_1 = x_2 = x_3$ in both quark and gluon jets, increasing as a function of $\ln(x_i/x_j)$ and $|\ln(x_i x_j)|$ when x_k softens, that is for partons being less sensitive to the energy balance.

Coherence effects appear when one or two of the partons involved in the process is harder than the others, thus reproducing for this observable the hump-backed shape of the one particle distribution. Away from the maximum at $x_i = x_i$, because of limitation of the phase space, one has $C^{(3)} \leq 1$. Predictions beyond the limiting spectrum for heavier charged hadrons as compared with pions and kaons show that the correlations should increase as the parameter Q_0 equals the mass of such hadrons and the range where $C^{(3)} \geq 1$ has been enlarged beyond this limit. The last statement is not surprising because soft gluon emission gets suppressed between the two scales Q_0 and Λ_{QCD} for $\lambda \neq 0$, thus decreasing the particle yield inside the whole jet. This measurement would in particular provide an additional and independent check of the LPHD for massive charged hadrons. As was shown in 2.4, the DLA solution of the evolution equations provide general features of the observable showing its unreliability to be compared with the experiment. That is why, the MLLA shape and overall normalization of this observable should be compared with the data. In the case of $p\bar{p}$ collisions at the Tevatron, since diet events consist of both gluon and quark jets, in order to compare data to theory, a parameter f_g for mixed samples of quark and gluon jets was chosen [11]. In pp collisions at the LHC, the same procedure can be applied so as to measure the two- and three-particle correlations. Furthermore, MLLA corrections have been shown to be larger for three than for two particles, that is to increase as the number of particles increases.

As was the case for two particles, the three-particle correlations are larger inside a quark than in a gluon jet. Same trends have been observed in HERA and LEP data for soft multi-particle fluctuations in [34,35]. Finally, we give the first analytical predictions for intra-jet three-particle correlations in view of forth-

coming measurements by ATLAS, CMS and ALICE at the LHC.

Acknowledgements

We gratefully acknowledge enlightening discussions with W. Ochs and E. Sarkisyan-Grinbau as well as support from Generalitat Valenciana under grant PROMETEO/2008/004 and M.A.S. from FPA2008-02878 and GVPROMETEO2010-056. V.M acknowledges support from the grant HadronPhysics2, a FP7-Integrating Activities and Infrastructure Program of the European Commission under Grant 227431, by UE (Feder) and the MICINN (Spain) grant FPA 2010-21750-C02-01.

A MLLA approximation

In (23a), for $\ln(1-z) \ll \ln x$ and $\ln z \ll \ln x$, we perform the following Taylor expansions:

$$Q^{(3)}(1-z) - Q^{(3)} \approx \ln(1-z) \frac{dQ^{(3)}}{d\ell_1} + \mathcal{O}(\alpha_s), \quad (71)$$

$$\begin{aligned} & \left(Q_{ij}^{(2)}(1-z) - Q_{ij}^{(2)} \right) (G_k(z) - Q_k) + \left(G_{ij}^{(2)}(z) - Q_{ij}^{(2)} \right) (Q_k(1-z) - Q_k) \\ &= \ln(1-z) \left[\frac{dQ_{ij}^{(2)}}{d\ell_1} (G_k - Q_k) + \left(G_{ij}^{(2)} - Q_{ij}^{(2)} \right) \frac{dQ_k}{d\ell_1} \right] + \mathcal{O}(\alpha_s), \end{aligned} \quad (72)$$

$$(Q_i - G_i(z)) (Q_j(1-z) - Q_j) Q_k \approx \ln(1-z) (Q_i - G_i) \frac{dQ_j}{d\ell_1} Q_k + \mathcal{O}(\alpha_s). \quad (73)$$

Since none of these terms contribute to MLLA $\mathcal{O}(\sqrt{\alpha_s})$, they will be dropped hereafter. In equation (23b), we perform the following approximations in the hard fragmentation region,

$$\left(G_{ij}^{(2)}(z) - G_{ij}^{(2)} \right) (G_k(1-z) - G_k) \approx \ln z \ln(1-z) \frac{dG_{ij}^{(2)}}{d\ell_1} \frac{G_k}{d\ell_1} + \mathcal{O}(\alpha_s), \quad (74)$$

$$(G_i - G_i(z))(G_j(1-z) - G_j)G_k \approx -\ln z \ln(1-z) \frac{dG_i}{d\ell_1} \frac{dG_j}{d\ell_1} G_k + \mathcal{O}(\alpha_s). \quad (75)$$

Neither (74) nor (75) contribute to MLLA. The other terms in (23b) can be written as,

$$2Q^{(3)}(z) - G^{(3)} \approx (2Q^{(3)} - G^{(3)}) + 2\ln z \frac{dQ^{(3)}}{d\ell_1} + \mathcal{O}(\alpha_s) \quad (76)$$

$$\begin{aligned} & 2 \left(Q_{ij}^{(2)}(z) - G_{ij}^{(2)} \right) (Q_k(1-z) - G_k) \approx 2 \left(Q_{ij}^{(2)} - G_{ij}^{(2)} \right) (Q_k - G_k) \\ & + 2\ln(1-z) \left(Q_{ij}^{(2)} - G_{ij}^{(2)} \right) \frac{dQ_k}{d\ell_1} + 2\ln z (Q_k - G_k) \frac{dQ_{ij}^{(2)}}{d\ell_1} + \mathcal{O}(\alpha_s), \end{aligned} \quad (77)$$

$$(2Q_i(z)Q_j(z) - G_iG_j)G_k \approx (2Q_iQ_j - G_iG_j)G_k + \ln z \left(Q_i \frac{dQ_j}{d\ell_1} + \frac{dQ_i}{d\ell_1} Q_j \right) + \mathcal{O}(\alpha_s), \quad (78)$$

$$(G_i - 2Q_i(z))(2Q_j(1-z) - G_j)G_k \approx (G_i - 2Q_i)(2Q_j - G_j)G_k - 2(2Q_j - G_j)G_k \ln z \frac{dQ_i}{d\ell_1} G_k$$

$$+ 2(G_i - 2Q_i) \ln(1 - z) \frac{dQ_j}{d\ell_1} G_k + \mathcal{O}(\alpha_s), \quad (79)$$

such that only the first terms in (76), (77), (78) and (79) will be kept in the following. Furthermore, we make use of the identity [19]

$$\int^1 dz \Phi_g^g(z) \left(G^{(3)}(z) - zG^{(3)} \right) = \int^1 dz (1 - z) \Phi_g^g(z) \left(G^{(3)}(z) + \left(G^{(3)}(z) - G^{(3)} \right) \right),$$

such that $G^{(n)}(z) - zG^{(n)}$ can be replaced by,

$$G^{(n)}(z) - zG^{(n)} \rightarrow (1 - z) \left[G^{(n)}(z) + \left(G^{(n)}(z) - G^{(n)} \right) \right] \approx (1 - z) \left[G^{(n)}(z) + \ln z \frac{dG^{(n)}}{d\ell_1} \right],$$

($n = 1, 2, 3$) in the r.h.s. of equations (21b), (22b) and (23b). Indeed, terms $\propto \ln z, \ln(1 - z)$ provide NMLLA corrections $\mathcal{O}(\alpha_s)$ which improve energy conservation; however, their inclusion goes beyond the scope of the present paper.

A.1 One and two particle distributions at small x

The MLLA integro-differential version of equations (21a,21b) and (22b,22a) is obtained after integrating over the regular part of the splitting functions, such that [6, 18, 19]

$$Q_{i,y} = \frac{C_F}{N_c} \int_0^\ell d\ell' \gamma_0^2(\ell' + y) G_i(\ell', y) - \frac{3}{4} \frac{C_F}{N_c} \gamma_0^2(\ell + y) G_i(\ell, y), \quad (80)$$

$$G_{i,y} = \int_0^\ell d\ell' \gamma_0^2(\ell' + y) G_i(\ell', y) - a \gamma_0^2(\ell + y) G_i(\ell, y), \quad (81)$$

with $\gamma_0^2(\ell + y) = \frac{1}{\beta_0(\ell + y + \lambda)}$, and the two-particle correlations ($\hat{A}_{ij}^{(2)} = A_{ij}^{(2)} - A_i A_j$) [18, 19],

$$\hat{Q}_{ij,y}^{(2)} = \frac{C_F}{N_c} \int_0^{\ell_i} d\ell \gamma_0^2(\ell + y_j) G_{ij}^{(2)}(\ell, y_j, \eta_{ij}) - \frac{3}{4} \frac{C_F}{N_c} \gamma_0^2(\ell_i + y_j) G_{ij}^{(2)}(\ell_i, y_j, \eta_{ij}), \quad (82)$$

$$\begin{aligned} \hat{G}_{ij,y}^{(2)} &= \int_0^{\ell_i} \gamma_0^2(\ell + y_j) G^{(2)}(\ell, y_j, \eta_{ij}) - a \gamma_0^2(\ell_i + y_j) G_{ij}^{(2)}(\ell_i, y_j, \eta_{ij}) \\ &\quad + (a - b) \gamma_0^2(\ell_i + y_j) G(\ell_i, y_j + \eta_{ij}) G(\ell_i + \eta_{ij}, y_j), \end{aligned} \quad (83)$$

with $\gamma_0^2(\ell_i + y_j) = \frac{1}{\beta_0(\ell_i + y_j + \eta_{ij} + \lambda)}$, after accounting for hard corrections $\mathcal{O}(\sqrt{\alpha_s})$. After differentiating (80,81) and (82,83) with respect to “ ℓ ”, one has [19]

$$Q_{i,\ell y} = \frac{C_F}{N_c} \gamma_0^2 G_i - \frac{C_F}{N_c} \frac{3}{4} \gamma_0^2 (G_{i,\ell} - \beta_0 \gamma_0^2 G_i), \quad (84)$$

$$G_{i,\ell y} = \gamma_0^2 G_i - a \gamma_0^2 (G_{i,\ell} - \beta_0 \gamma_0^2 G_i), \quad (85)$$

from where the following useful relations hold in MLLA [19],

$$\frac{Q_{i,\ell y}}{\gamma_0^2 Q_i} = \left[1 - \frac{3}{4} \psi_{i,\ell} \right] \frac{C_F}{N_c} \frac{G_i}{Q_i} + \mathcal{O}(\gamma_0^2), \quad (86)$$

$$\frac{G_i}{Q_i} = \frac{N_c}{C_F} \left[1 - \left(a - \frac{3}{4} \right) \psi_{i,\ell} \right] + \mathcal{O}(\gamma_0^2), \quad (87)$$

$$\frac{Q_{i,\ell y}}{\gamma_0^2 Q_i} = 1 - a \psi_{i,\ell} + \mathcal{O}(\gamma_0^2). \quad (88)$$

Corrections $\propto \beta_0$ in (84) and (85), which are NMLLA, account for the running of the coupling constant α_s and those $\propto \frac{3}{4}, a, (a-b)$ account for energy conservation in the hard parton splitting region. The MLLA gluon inclusive spectrum is given by the solution of (85) [6] and can be written in the form [14]:

$$G_i(\ell, y) = 2 \frac{\Gamma(B)}{\beta_0} \int_0^{\frac{\pi}{2}} \frac{d\tau}{\pi} e^{-B\alpha} \mathcal{F}_B(\tau, y, \ell), \quad (89)$$

where the integration is performed with respect to τ defined by $\alpha = \frac{1}{2} \ln \frac{y}{\ell} + i\tau$ and with

$$\mathcal{F}_B(\tau, y, \ell) = \left[\frac{\cosh \alpha - \frac{y-\ell}{y+\ell} \sinh \alpha}{\frac{\ell+y}{\beta_0} \frac{\alpha}{\sinh \alpha}} \right]^{B/2} I_B(2\sqrt{Z(\tau, y, \ell)}),$$

$$Z(\tau, y, \ell) = \frac{\ell+y}{\beta_0} \frac{\alpha}{\sinh \alpha} \left(\cosh \alpha - \frac{y-\ell}{y+\ell} \sinh \alpha \right),$$

$B = a/\beta_0$ and I_B is the modified Bessel function of the first kind. The formula in (89) corresponds indeed to the so-called hump-backed plateau, which describes the energy spectrum of soft hadrons in the limiting spectrum approximation $Q_0 = \Lambda_{QCD}$ [6, 28]. This result is well known and constitutes one of the strikest predictions of pQCD. The corresponding solution of (84) for $Q_i(\ell, y)$ can be obtained from (87) with accuracy $\mathcal{O}(\sqrt{\alpha_s})$. The system of differential evolution equations for two-particle correlations follows from (82) and (83), such that [19]

$$\left[Q_{ij}^{(2)} - Q_i Q_j \right]_{\ell y} = \frac{C_F}{N_c} \gamma_0^2 G_{ij}^{(2)} - \frac{3}{4} \frac{C_F}{N_c} \gamma_0^2 \left(G_{ij,\ell}^{(2)} - \beta_0 \gamma_0^2 G_{ij}^{(2)} \right), \quad (90)$$

$$\left[G_{ij}^{(2)} - G_i G_j \right]_{\ell y} = \gamma_0^2 G_{ij}^{(2)} - a \gamma_0^2 \left(G_{ij,\ell}^{(2)} - \beta_0 \gamma_0^2 G_{ij}^{(2)} \right) + (a-b) \gamma_0^2 \left[(G_i G_j)_\ell - \beta_0 \gamma_0^2 G_i G_j \right]. \quad (91)$$

In [19], the system (82,83) was solved iteratively after replacing $G_{ij}^{(2)} = C_{G,ij}^{(2)} G_i G_j$ and $Q_{ij}^{(2)} = C_{Q,ij}^{(2)} Q_i Q_j$ in (91) and (90) respectively. The MLLA solutions of (90) and (91), which are to be used in the present paper read [19]

$$\mathcal{C}_{G_{ij}}^{(2)} - 1 = \frac{1 - \delta_1^{ij} - b(\psi_{i,\ell} + \psi_{j,\ell})}{1 + \Delta_{ij} + \delta_1^{ij}}, \quad (92)$$

$$\frac{\mathcal{C}_{Q_{ij}}^{(2)} - 1}{\mathcal{C}_{G_{ij}}^{(2)} - 1} = \frac{N_c}{C_F} \left[1 + (b-a)(\psi_{i,\ell} + \psi_{j,\ell}) \frac{1 + \Delta_{ij}}{2 + \Delta_{ij}} \right], \quad (93)$$

which were evaluated by the steepest descent method over the single inclusive distribution in [25]. We have introduced the following notations and functions [19],

$$\Delta_{ij} = \gamma_0^{-2} (\psi_{i,\ell} \psi_{j,y} + \psi_{i,y} \psi_{j,\ell}) = \mathcal{O}(1); \quad (94)$$

$$\chi^{ij} = \ln \dot{\mathcal{C}}_{G_{ij}}^{(2)} = \mathcal{O}(1), \quad \chi_\ell^{ij} = \frac{\partial \chi^{ij}}{\partial \ell} = \mathcal{O}(\gamma_0^2), \quad \chi_y = \frac{\partial \chi^{ij}}{\partial y} = \mathcal{O}(\gamma_0^2); \quad (95)$$

$$\delta_1^{ij} = \gamma_0^{-2} \left[\chi_\ell^{ij} (\psi_{i,y} + \psi_{j,y}) + \chi_y^{ij} (\psi_{j,\ell} + \psi_{i,\ell}) \right] = \mathcal{O}(\gamma_0), \quad (96)$$

where, following from (38) and (39), we have evaluated the corresponding order of magnitude of these quantities in powers of the anomalous dimension $\gamma_0 \propto \sqrt{\alpha_s}$. The solution is iterative with respect to corrections χ and δ_1 , which need the prior evaluation of the DLA solution $\dot{\mathcal{C}}_{G_{ij}}^{(2)}$ of the equations.

B Iterative solution of the evolution equations

Let us first solve the equation (50). For the sake of simplicity, it is much easier to solve the equivalent equation:

$$\begin{aligned} \hat{G}_{\ell y}^{(3)} = & \gamma_0^2 G^{(3)} - a\gamma_0^2 \left(G_\ell^{(3)} - \beta_0 \gamma_0^2 G^{(3)} \right) + (a-b)\gamma_0^2 \left\{ \left[G_{12}^{(2)} G_3 + G_{13}^{(2)} G_2 + G_{23}^{(2)} G_1 \right]_\ell \right. \\ & \left. - \beta_0 \gamma_0^2 \left[G_{12}^{(2)} G_3 + G_{13}^{(2)} G_2 + G_{23}^{(2)} G_1 \right] \right\} + (2a-3b+c)\gamma_0^2 \left[(G_1 G_2 G_3)_\ell - \beta_0 \gamma_0^2 G_1 G_2 G_3 \right]. \end{aligned} \quad (97)$$

One has to substitute the following in the l.h.s. of the equation (97):

$$G^{(3)} = \mathcal{C}_{G_{123}}^{(3)} G_1 G_2 G_3, \quad G_{ij}^{(2)} = \mathcal{C}_{G_{ij}}^{(2)} G_i G_j.$$

Thus, after normalizing by $\gamma_0^2 G_1 G_2 G_3$, one finds,

$$\begin{aligned} \frac{\left[(\mathcal{C}_{G_{123}}^{(3)} - 1) G_1 G_2 G_3 \right]_{\ell y}}{\gamma_0^2 G_1 G_2 G_3} = & \mathcal{C}_{G_{123}}^{(3)} (\epsilon_1 + \epsilon_2) + (\mathcal{C}_{G_{123}}^{(3)} - 1) [3 + \Delta_{12} + \Delta_{13} + \Delta_{23} \\ & - a(\psi_{1,\ell} + \psi_{2,\ell} + \psi_{3,\ell}) + 3a\beta_0 \gamma_0^2], \end{aligned} \quad (98)$$

while for the other terms in the r.h.s. of the same equation one finds,

$$\begin{aligned} \frac{\left[(\mathcal{C}_{G_{ij}}^{(2)} - 1) G_1 G_2 G_3 \right]_{\ell y}}{\gamma_0^2 G_1 G_2 G_3} = & (\mathcal{C}_{G_{ij}}^{(2)} - 1) \left(\sum_{i=1}^3 \frac{G_{i,\ell y}}{\gamma_0^2 G_i} + \Delta_{12} + \Delta_{13} + \Delta_{23} \right) + \mathcal{C}_{G_{ij}}^{(2)} \xi_1^{ij} + \mathcal{C}_{G_{ij}}^{(2)} \delta_2^{ij} \\ = & (\mathcal{C}_{G_{ij}}^{(2)} - 1) [3 + \Delta_{12} + \Delta_{13} + \Delta_{23} - a(\psi_{1,\ell} + \psi_{2,\ell} + \psi_{3,\ell}) + 3a\beta_0 \gamma_0^2 \\ & + \xi_1^{ij} + \delta_2^{ij}] + \xi_1^{ij} + \delta_2^{ij}. \end{aligned} \quad (99)$$

The r.h.s. provides the following contribution

$$\begin{aligned} \frac{r.h.s.}{\gamma_0^2 G_1 G_2 G_3} = & \mathcal{C}_{G_{123}}^{(3)} - a\mathcal{C}_{G_{123}}^{(3)} (\psi_{1,\ell} + \psi_{2,\ell} + \psi_{3,\ell} + \zeta_\ell - \beta_0 \gamma_0^2) + (a-b) \left[\mathcal{C}_{G_{12}}^{(2)} (\chi_\ell^{12} + \psi_{1,\ell} + \psi_{2,\ell} \right. \\ & + \psi_{3,\ell}) + \mathcal{C}_{G_{13}}^{(2)} (\chi_\ell^{13} + \psi_{1,\ell} + \psi_{2,\ell} + \psi_{3,\ell}) + \mathcal{C}_{G_{23}}^{(2)} (\chi_\ell^{23} + \psi_{1,\ell} + \psi_{2,\ell} + \psi_{3,\ell}) \\ & \left. - \beta_0 \gamma_0^2 (\mathcal{C}_{G_{12}}^{(2)} + \mathcal{C}_{G_{13}}^{(2)} + \mathcal{C}_{G_{23}}^{(2)}) \right] + (3b-2a-c)(\psi_{1,\ell} + \psi_{2,\ell} + \psi_{3,\ell} - \beta_0 \gamma_0^2). \end{aligned} \quad (100)$$

After adding (98) and (99) and equating with (100) together with some algebra in between, one finds the solution written in (51). Following the same iterative procedure

$$Q^{(3)} = \mathcal{C}_{Q_{123}}^{(3)} Q_1 Q_2 Q_3, \quad Q_{ij}^{(2)} = \mathcal{C}_{Q_{ij}}^{(2)} Q_i Q_j; \quad G^{(3)} = \mathcal{C}_{G_{123}}^{(3)} G_1 G_2 G_3,$$

for the quark jet evolution equation written in (49), one has,

$$\begin{aligned} & \left(\mathcal{C}_{Q_{123}}^{(3)} - 1 \right) \left(\tilde{\Delta}_{12} + \tilde{\Delta}_{13} + \tilde{\Delta}_{23} + \sum_{i=1}^3 \frac{Q_{i,\ell y}}{\gamma_0^2 Q_i} + \tilde{\epsilon}_1 + \tilde{\epsilon}_2 \right) \\ & - \left(\mathcal{C}_{Q_{12}}^{(2)} - 1 \right) \left(\tilde{\Delta}_{12} + \tilde{\Delta}_{13} + \tilde{\Delta}_{23} + \sum_{i=1}^3 \frac{Q_{i,\ell y}}{\gamma_0^2 Q_i} + \tilde{\xi}_1^{12} + \tilde{\delta}_2^{12} \right) \\ & - \left(\mathcal{C}_{Q_{13}}^{(2)} - 1 \right) \left(\tilde{\Delta}_{12} + \tilde{\Delta}_{13} + \tilde{\Delta}_{23} + \sum_{i=1}^3 \frac{Q_{i,\ell y}}{\gamma_0^2 Q_i} + \tilde{\xi}_1^{13} + \tilde{\delta}_2^{13} \right) \\ & - \left(\mathcal{C}_{Q_{23}}^{(2)} - 1 \right) \left(\tilde{\Delta}_{12} + \tilde{\Delta}_{13} + \tilde{\Delta}_{23} + \sum_{i=1}^3 \frac{Q_{i,\ell y}}{\gamma_0^2 Q_i} + \tilde{\xi}_1^{23} + \tilde{\delta}_2^{23} \right) \end{aligned} \quad (101)$$

$$= \frac{C_F}{N_c} \mathcal{C}_{G_{123}}^{(3)} \left[1 - \frac{3}{4} (\psi_{1,\ell} + \psi_{2,\ell} + \psi_{3,\ell} + \zeta_\ell - \beta_0 \gamma_0^2) \right] \frac{G_1 G_2 G_3}{Q_1 Q_2 Q_3} \\ + (\tilde{\xi}_1^{12} + \tilde{\delta}_2^{12}) + (\tilde{\xi}_1^{13} + \tilde{\delta}_2^{13}) + (\tilde{\xi}_1^{23} + \tilde{\delta}_2^{23}) - \tilde{\epsilon}_1 - \tilde{\epsilon}_2.$$

Finally by adding and subtracting $(\tilde{\epsilon}_1 + \tilde{\epsilon}_2)$ in every term $\propto (\mathcal{C}_{Q_{ij}}^{(2)} - 1)$ in the l.h.s. of (101) one finds (55).

C Steepest descent evaluation: reminder from [25]

The evaluation of the integral representation by the steepest descent method at small $x \ll 1$ (or large $\ell \gg 1$) and very high energy $Y \gg 1$ leads to the result,

$$G(\ell, y) \approx \mathcal{N}(\mu, \nu, \lambda) \exp \left[\frac{2}{\beta_0} \left(\sqrt{\ell + y + \lambda} - \sqrt{\lambda} \right) \frac{\mu - \nu}{\sinh \mu - \sinh \nu} + \nu - \frac{a}{\beta_0} (\mu - \nu) \right], \quad (102)$$

where

$$\mathcal{N}(\mu, \nu, \lambda) = \frac{1}{2} (\ell + y + \lambda) \frac{\left(\frac{\beta_0}{\lambda} \right)^{1/4}}{\sqrt{\pi \cosh \nu \text{Det} A(\mu, \nu)}},$$

with

$$\text{Det} A(\mu, \nu) = \beta_0 (\ell + y + \lambda)^3 \left[\frac{(\mu - \nu) \cosh \mu \cosh \nu + \cosh \mu \sinh \nu - \sinh \mu \sinh \nu}{\sinh^3 \mu \cosh \nu} \right].$$

The logarithmic derivatives of the spectrum given in (65) and (66) were derived from (102) and it was also shown that (102) reproduces the Gaussian shape of the inclusive distribution near the hump $\ell_{max} \approx Y/2$. From (102), one has indeed,

$$G(\ell, y) \approx \left(\frac{3}{\pi \sqrt{\beta_0} [(\ell + y + \lambda)^{3/2} - \lambda^{3/2}]} \right)^{1/2} \exp \left(- \frac{2}{\sqrt{\beta_0}} \frac{3}{(\ell + y + \lambda)^{3/2} - \lambda^{3/2}} \frac{(\ell - Y/2)^2}{2} \right), \quad (103)$$

where the MLLA ℓ_{max} reads,

$$\ell_{max} \approx \frac{Y}{2} + \frac{1}{2} \frac{a}{\beta_0} \left(\sqrt{Y + \lambda} - \sqrt{\lambda} \right).$$

Setting $a = 0$ and $\lambda = 0$ in the previous expressions one recovers the DLA results, which are needed for subsection 2.4. The functions entering as a function of (μ, ν) in (65) and (66) are the following,

$$\tilde{Q}(\mu, \nu) = \frac{\cosh \mu \sinh \mu \cosh \nu - (\mu - \nu) \cosh \nu - \sinh \nu}{(\mu - \nu) \cosh \mu \cosh \nu + \cosh \mu \sinh \nu - \sinh \mu \cosh \nu}, \quad (104)$$

$$K(\mu, \nu) = -\frac{1}{2} \sinh \nu \frac{(\mu - \nu) \cosh \mu - \sinh \mu}{(\mu - \nu) \cosh \mu \cosh \nu + \cosh \mu \sinh \nu - \sinh \mu \cosh \nu}, \quad (105)$$

$$L(\mu, \nu) = \frac{3}{2} \coth \mu - \frac{1}{2} \frac{(\mu - \nu) \cosh \nu \sinh \mu + \sinh \nu \sinh \mu}{(\mu - \nu) \cosh \mu \cosh \nu + \cosh \mu \sinh \nu - \sinh \mu \cosh \nu}, \quad (106)$$

$$C(\mu, \nu) = L(\mu, \nu) + \tanh \nu \coth \mu (1 + K(\mu, \nu)). \quad (107)$$

The expressions for the two particle correlations follow from (92) and (93) [25],

$$\mathcal{C}_{G_{ij}}^{(2)} = 1 + \frac{1 - b\gamma_0(e^{\mu_i} + e^{\mu_j}) - \delta_1^{ij}}{1 + 2 \cosh(\mu_i - \mu_j) + \Delta'(\mu_i, \nu_i, \mu_j, \nu_j) + \delta_1^{ij}}, \quad (108)$$

$$\mathcal{C}_{Q_{ij}}^{(2)} = 1 + \frac{N_c}{C_F} \left[\mathcal{C}_{G_{ij}}^{(2)} - 1 + \frac{1}{2} (b - a) \gamma_0 \frac{e^{\mu_i} + e^{\mu_j}}{1 + \cosh(\mu_i - \mu_j)} \right], \quad (109)$$

where,

$$\delta_1^{ij} = \beta_0 \gamma_0 \frac{2 \sinh^2 \left(\frac{\mu_i - \mu_j}{2} \right)}{3 + 4 \sinh^2 \left(\frac{\mu_i - \mu_j}{2} \right)} \left(\tilde{Q}(\mu_i, \nu_i) + \tilde{Q}(\mu_j, \nu_j) \right), \quad (110)$$

and

$$\begin{aligned} \Delta'(\mu_i, \nu_i, \mu_j, \nu_j) = & -a\gamma_0 \left[e^{\mu_i} + e^{\mu_j} - \sinh(\mu_i - \mu_j)(\tilde{Q}_i - \tilde{Q}_j) + \cosh \mu_1 \tanh \nu_2 + \cosh \mu_2 \tanh \nu_1 \right. \\ & - \sinh \mu_i \tanh \nu_j \coth \mu_j - \sinh \mu_j \tanh \nu_i \coth \mu_i \\ & \left. + \sinh(\mu_i - \mu_j) \left(\tanh \nu_i \coth \mu_i \tilde{Q}_i - \tanh \nu_j \coth \mu_j \tilde{Q}_j \right) \right] \\ & - \beta_0 \gamma_0 \left[\cosh \mu_i - \sinh \mu_i C_j + \cosh \mu_j - \sinh \mu_j C_i + \sinh(\mu_i - \mu_j)(C_i \tilde{Q}_i - C_j \tilde{Q}_j) \right. \\ & \left. + \cosh \mu_i \tanh \nu_j (1 + K_j) + \cosh \mu_j \tanh \nu_i (1 + K_i) \right]. \end{aligned} \quad (111)$$

The solutions (108) and (109) are the ones to be used in this paper for the evaluations of the three-particle correlations and will be directly inserted in the solutions (51) and (55) respectively.

C.1 Corrections ξ_1^{ij} , $\tilde{\xi}_1^{ij}$ and $\epsilon_1, \tilde{\epsilon}_1$

For the computation of these corrections, one only needs to take the DLA part of the logarithmic derivatives of the one-particle distribution $\psi_{i,\ell} = \gamma_0 e^{\mu_i}$ and $\psi_{i,y} = \gamma_0 e^{-\mu_i}$, such that after replacement in (54c) and (58c) one finds,

$$\xi_1^{ij} = \frac{1}{\gamma_0} \left[\chi_\ell^{ij} (e^{-\mu_1} + e^{-\mu_2} + e^{-\mu_3}) + \chi_y^{ij} (e^{\mu_1} + e^{\mu_2} + e^{\mu_3}) \right], \quad (112)$$

$$\tilde{\xi}_1^{ij} = \frac{1}{\gamma_0} \left[\tilde{\chi}_\ell^{ij} (e^{-\mu_1} + e^{-\mu_2} + e^{-\mu_3}) + \tilde{\chi}_y^{ij} (e^{\mu_1} + e^{\mu_2} + e^{\mu_3}) \right], \quad (113)$$

where

$$\chi_\ell^{ij} = \beta_0 \gamma_0^2 \frac{\tanh \frac{\mu_i - \mu_j}{2}}{1 + 2 \cosh(\mu_i - \mu_j)} \frac{e^{\mu_i} \tilde{Q}_i - e^{\mu_j} \tilde{Q}_j}{2}, \quad \tilde{\chi}_\ell^{ij} = -\frac{N_c}{C_F} \frac{\dot{C}_{G_{ij}}^{(2)}}{\dot{C}_{Q_{ij}}^{(2)}} \chi_\ell^{ij}, \quad (114)$$

$$\chi_y^{ij} = -\beta_0 \gamma_0^2 \frac{\tanh \frac{\mu_i - \mu_j}{2}}{1 + 2 \cosh(\mu_i - \mu_j)} \frac{e^{-\mu_i} \tilde{Q}_i - e^{-\mu_j} \tilde{Q}_j}{2}, \quad \tilde{\chi}_y^{ij} = -\frac{N_c}{C_F} \frac{\dot{C}_{G_{ij}}^{(2)}}{\dot{C}_{Q_{ij}}^{(2)}} \chi_y^{ij}; \quad (115)$$

with

$$\dot{C}_{G_{ij}}^{(2)} = 1 + \frac{1}{1 + 2 \cosh(\mu_i - \mu_j)}, \quad \dot{C}_{Q_{ij}}^{(2)} = 1 + \frac{N_c}{C_F} \frac{1}{1 + 2 \cosh(\mu_i - \mu_j)}. \quad (116)$$

Accordingly, replacing $\psi_{i,\ell} = \gamma_0 e^{\mu_i}$ and $\psi_{i,y} = \gamma_0 e^{-\mu_i}$ in (54e) and (58e), one has

$$\epsilon_1 = \frac{1}{\gamma_0} \left[\zeta_\ell (e^{-\mu_1} + e^{-\mu_2} + e^{-\mu_3}) + \zeta_y (e^{\mu_1} + e^{\mu_2} + e^{\mu_3}) \right], \quad (117)$$

$$\tilde{\epsilon}_1 = \frac{1}{\gamma_0} \left[\tilde{\zeta}_\ell (e^{-\mu_1} + e^{-\mu_2} + e^{-\mu_3}) + \tilde{\zeta}_y (e^{\mu_1} + e^{\mu_2} + e^{\mu_3}) \right], \quad (118)$$

where $\zeta_\ell, \tilde{\zeta}_\ell$ and $\zeta_y, \tilde{\zeta}_y$ should be found from the DLA expression of $\mathcal{C}^{(3)}$ written in (35), for $C_A = N_c$ in a gluon jet and $C_A = C_F$ in a quark jet. Introducing the parametrization in (μ, ν) , one has respectively,

$$\begin{aligned} \dot{C}_{G_{123}}^{(3)} = & 1 + \left(\dot{C}_{G_{12}}^{(2)} - 1 \right) + \left(\dot{C}_{G_{13}}^{(2)} - 1 \right) + \left(\dot{C}_{G_{23}}^{(2)} - 1 \right) \\ & + \frac{1}{2} \frac{\left(\dot{C}_{G_{12}}^{(2)} - 1 \right) + \left(\dot{C}_{G_{13}}^{(2)} - 1 \right) + \left(\dot{C}_{G_{23}}^{(2)} - 1 \right)}{1 + \cosh(\mu_1 - \mu_2) + \cosh(\mu_1 - \mu_3) + \cosh(\mu_2 - \mu_3)} \end{aligned} \quad (119)$$

$$+ \frac{1}{2} \frac{1}{1 + \cosh(\mu_1 - \mu_2) + \cosh(\mu_1 - \mu_3) + \cosh(\mu_2 - \mu_3)},$$

and

$$\begin{aligned} \dot{C}_{Q_{123}}^{(3)} &= 1 + \left(\dot{C}_{Q_{12}}^{(2)} - 1 \right) + \left(\dot{C}_{Q_{13}}^{(2)} - 1 \right) + \left(\dot{C}_{Q_{23}}^{(2)} - 1 \right) \\ &+ \frac{N_c}{2C_F} \frac{\left(\dot{C}_{Q_{12}}^{(2)} - 1 \right) + \left(\dot{C}_{Q_{13}}^{(2)} - 1 \right) + \left(\dot{C}_{Q_{23}}^{(2)} - 1 \right)}{1 + \cosh(\mu_1 - \mu_2) + \cosh(\mu_1 - \mu_3) + \cosh(\mu_2 - \mu_3)} \\ &+ \frac{N_c^2}{2C_F^2} \frac{1}{1 + \cosh(\mu_1 - \mu_2) + \cosh(\mu_1 - \mu_3) + \cosh(\mu_2 - \mu_3)}. \end{aligned} \quad (120)$$

Thus, in order to get ζ_ℓ and ζ_y , one should start from (119,120) and make use of

$$\frac{\partial \mu_i}{\partial \ell} - \frac{\partial \mu_j}{\partial \ell} = -\beta_0 \gamma_0^2 \frac{e^{\mu_i} \tilde{Q}_i - e^{\mu_j} \tilde{Q}_j}{2}, \quad \frac{\partial \mu_i}{\partial y} - \frac{\partial \mu_j}{\partial y} = \beta_0 \gamma_0^2 \frac{e^{-\mu_i} \tilde{Q}_i - e^{-\mu_j} \tilde{Q}_j}{2}.$$

Therefore, everything is ready for the computation of

$$\zeta_\ell = \frac{1}{\dot{C}_{G_{123}}^{(3)}} \dot{C}_{G_{123,\ell}}^{(3)}, \quad \zeta_y = \frac{1}{\dot{C}_{G_{123}}^{(3)}} \dot{C}_{G_{123,y}}^{(3)}, \quad \tilde{\zeta}_\ell = \frac{1}{\dot{C}_{Q_{123}}^{(3)}} \dot{C}_{Q_{123,\ell}}^{(3)}, \quad \tilde{\zeta}_y = \frac{1}{\dot{C}_{Q_{123}}^{(3)}} \dot{C}_{Q_{123,y}}^{(3)}. \quad (121)$$

For instance,

$$\begin{aligned} \dot{C}_{G_{123,\ell}}^{(3)} &= \chi_\ell^{12} \dot{C}_{G_{12}}^{(2)} + \chi_\ell^{13} \dot{C}_{G_{13}}^{(2)} + \chi_\ell^{23} \dot{C}_{G_{23}}^{(2)} + \frac{1}{2} \frac{\chi_\ell^{12} \dot{C}_{G_{12}}^{(2)} + \chi_\ell^{13} \dot{C}_{G_{13}}^{(2)} + \chi_\ell^{23} \dot{C}_{G_{23}}^{(2)}}{1 + \cosh(\mu_1 - \mu_2) + \cosh(\mu_1 - \mu_3) + \cosh(\mu_2 - \mu_3)} \\ &- \frac{1}{2} \frac{\left(\dot{C}_{G_{12}}^{(2)} - 1 \right) + \left(\dot{C}_{G_{13}}^{(2)} - 1 \right) + \left(\dot{C}_{G_{23}}^{(2)} - 1 \right)}{[1 + \cosh(\mu_1 - \mu_2) + \cosh(\mu_1 - \mu_3) + \cosh(\mu_2 - \mu_3)]^2} \left[\sinh(\mu_1 - \mu_2) \left(\frac{\partial \mu_1}{\partial \ell} - \frac{\partial \mu_2}{\partial \ell} \right) \right. \\ &+ \sinh(\mu_1 - \mu_3) \left(\frac{\partial \mu_1}{\partial \ell} - \frac{\partial \mu_3}{\partial \ell} \right) + \sinh(\mu_2 - \mu_3) \left(\frac{\partial \mu_2}{\partial \ell} - \frac{\partial \mu_3}{\partial \ell} \right) \Big] \\ &- \frac{1}{2} \frac{1}{[1 + \cosh(\mu_1 - \mu_2) + \cosh(\mu_1 - \mu_3) + \cosh(\mu_2 - \mu_3)]^2} \left[\sinh(\mu_1 - \mu_2) \left(\frac{\partial \mu_1}{\partial \ell} - \frac{\partial \mu_2}{\partial \ell} \right) \right. \\ &+ \sinh(\mu_1 - \mu_3) \left(\frac{\partial \mu_1}{\partial \ell} - \frac{\partial \mu_3}{\partial \ell} \right) + \sinh(\mu_2 - \mu_3) \left(\frac{\partial \mu_2}{\partial \ell} - \frac{\partial \mu_3}{\partial \ell} \right) \Big], \end{aligned} \quad (122)$$

and

$$\begin{aligned} \dot{C}_{Q_{123,\ell}}^{(3)} &= \tilde{\chi}_\ell^{12} \dot{C}_{Q_{12}}^{(2)} + \tilde{\chi}_\ell^{13} \dot{C}_{Q_{13}}^{(2)} + \tilde{\chi}_\ell^{23} \dot{C}_{Q_{23}}^{(2)} + \frac{N_c}{2C_F} \frac{\tilde{\chi}_\ell^{12} \dot{C}_{Q_{12}}^{(2)} + \tilde{\chi}_\ell^{13} \dot{C}_{Q_{13}}^{(2)} + \tilde{\chi}_\ell^{23} \dot{C}_{Q_{23}}^{(2)}}{1 + \cosh(\mu_1 - \mu_2) + \cosh(\mu_1 - \mu_3) + \cosh(\mu_2 - \mu_3)} \\ &- \frac{N_c}{2C_F} \frac{\left(\dot{C}_{Q_{12}}^{(2)} - 1 \right) + \left(\dot{C}_{Q_{13}}^{(2)} - 1 \right) + \left(\dot{C}_{Q_{23}}^{(2)} - 1 \right)}{[1 + \cosh(\mu_1 - \mu_2) + \cosh(\mu_1 - \mu_3) + \cosh(\mu_2 - \mu_3)]^2} \left[\sinh(\mu_1 - \mu_2) \left(\frac{\partial \mu_1}{\partial \ell} - \frac{\partial \mu_2}{\partial \ell} \right) \right. \\ &+ \sinh(\mu_1 - \mu_3) \left(\frac{\partial \mu_1}{\partial \ell} - \frac{\partial \mu_3}{\partial \ell} \right) + \sinh(\mu_2 - \mu_3) \left(\frac{\partial \mu_2}{\partial \ell} - \frac{\partial \mu_3}{\partial \ell} \right) \Big] \\ &- \frac{N_c^2}{2C_F^2} \frac{1}{[1 + \cosh(\mu_1 - \mu_2) + \cosh(\mu_1 - \mu_3) + \cosh(\mu_2 - \mu_3)]^2} \left[\sinh(\mu_1 - \mu_2) \left(\frac{\partial \mu_1}{\partial \ell} - \frac{\partial \mu_2}{\partial \ell} \right) \right. \\ &+ \sinh(\mu_1 - \mu_3) \left(\frac{\partial \mu_1}{\partial \ell} - \frac{\partial \mu_3}{\partial \ell} \right) + \sinh(\mu_2 - \mu_3) \left(\frac{\partial \mu_2}{\partial \ell} - \frac{\partial \mu_3}{\partial \ell} \right) \Big]. \end{aligned} \quad (123)$$

For derivatives with respect to y , it is enough to replace ℓ by y in the previous expressions. In Fig.8, we display $\epsilon_1(\ell_1, \ell_2, \ell_3, Y)$ as a function of the sum $|\ln(x_1 x_2)|$ and the difference $(\ell_1 - \ell_2) = \ln(x_2/x_1)$ for two fixed values of $\ell_3 = \ln(1/x_3) = 4.5, 5.5$, $x_1 = x_2$ and fixed sum $(\ell_1 + \ell_2) = |\ln(x_1 x_2)| = 10$ and fixed $Y = 7.5$. As expected, this correction decreases the correlations away from the hum region and for harder particles.

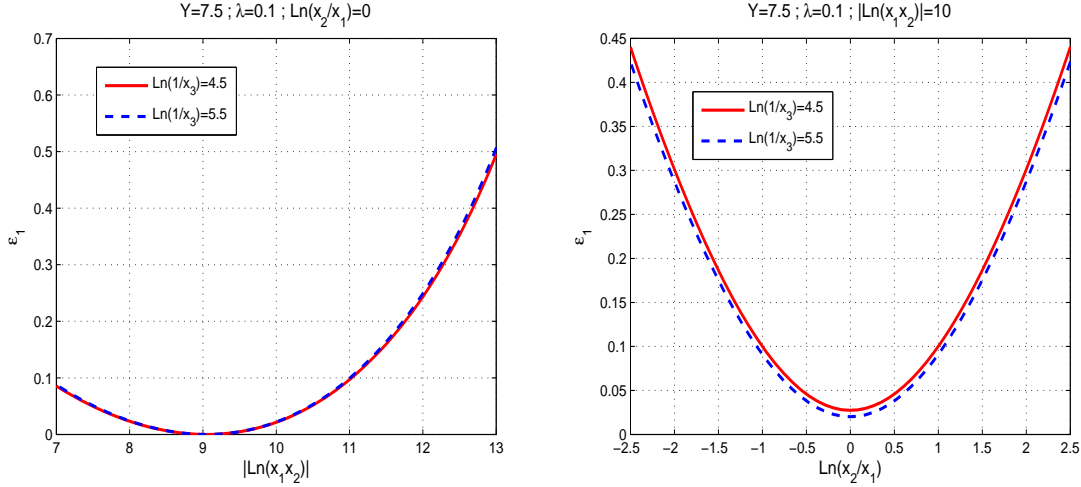


Figure 8: Correction $\epsilon_1(\ell_1, \ell_2, \ell_3, Y)$ as a function of $\ell_1 - \ell_2 = \ln(x_2/x_1)$ for $\ell_1 + \ell_2 = |\ln(x_1 x_2)| = 10$, $\ell_3 = \ln(1/x_3) = 4.5, 5.5$, fixed $Y = 7.5$ in the limiting spectrum approximation $\lambda \approx 0$.

C.2 Hump approximation

In this approximation, we consider the energy of the three partons to be close to the maximum of the single inclusive distribution $|\ell - Y/2| \ll \sigma \propto Y^{3/2}$ for $i = 1, 2, 3$. In [25], it was demonstrated that,

$$\psi_{i,\ell}^{\ell_i \sim Y/2} \approx \gamma_0(1 + \mu_i + \frac{1}{2}\mu_i^2), \quad \psi_{i,y}^{\ell_{i,j} \sim Y/2} \approx \gamma_0(1 - \mu_i + \frac{1}{2}\mu_j^2), \quad \mu_i^{\ell_i \sim Y/2} \approx \frac{3}{2} \frac{y - \ell}{y + \ell}, \quad (124)$$

for $a, \beta_0, \lambda = 0$, which is DLA. In the same approximation one has the following for $a, \beta_0 \neq 0$ and $\lambda = 0$,

$$\Delta_{ij}^{\ell_{i,j} \sim Y/2} \approx 2 + (\mu_i - \mu_j)^2 - a\gamma_0(2 + \mu_i + \mu_j) - 2\beta_0\gamma_0, \quad (125)$$

where

$$(\mu_i - \mu_j)^2 \approx 9 \left(\frac{\ell_i - \ell_j}{Y} \right)^2, \quad \mu_i + \mu_j \approx 3 \left(1 - \frac{\ell_i + \ell_j}{Y} \right). \quad (126)$$

Moreover,

$$\delta_1^{ij \ell_i \sim Y/2} \approx \frac{2}{9} \beta_0 \gamma_0 (\mu_i - \mu_j)^2 = 2\beta_0 \gamma_0 \left(\frac{\ell_i - \ell_j}{Y} \right)^2, \quad (127)$$

since $\gamma_0 \left(\frac{\ell_i - \ell_j}{Y} \right)^2 \ll \left(\frac{\ell_i - \ell_j}{Y} \right)^2$, δ_1 was neglected in this approximation.

Applying the previous expansions to (53a-53d) and (57a-57d), it is easy to find:

$$N_{Q_{ij}}^{(2)} = 0, \quad (128a)$$

$$N_G^{(3)} = 1 - \frac{3c}{\sqrt{\beta_0}} \left(\frac{5}{2} - \frac{|\ln(x_1 x_2 x_3)|}{\ln(Q/Q_0)} \right) \frac{1}{\sqrt{\ln(Q/Q_0)}} = 1 - 3c \left(\frac{5}{2} - \frac{\ell_1 + \ell_2 + \ell_3}{Y} \right) \gamma_0, \quad (128b)$$

$$\begin{aligned} D_G^{(3)} &= D_G^{(2)} = 8 + 9 \left[\frac{\ln(x_2/x_1)}{\ln(Q/Q_0)} \right]^2 + 9 \left[\frac{\ln(x_3/x_1)}{\ln(Q/Q_0)} \right]^2 + 9 \left[\frac{\ln(x_3/x_2)}{\ln(Q/Q_0)} \right]^2 - \frac{6\beta_0}{\sqrt{\beta_0 \ln(Q/Q_0)}}, \\ &\quad - \frac{3a}{\sqrt{\beta_0}} \left(5 - 2 \frac{|\ln(x_1 x_2 x_3)|}{\ln(Q/Q_0)} \right) \frac{1}{\sqrt{\ln(Q/Q_0)}}, \\ &= 8 + 9 \left(\frac{\ell_1 - \ell_2}{Y} \right)^2 + 9 \left(\frac{\ell_1 - \ell_3}{Y} \right)^2 + 9 \left(\frac{\ell_2 - \ell_3}{Y} \right)^2 - 6\beta_0 \gamma_0 - 3a \left(5 - 2 \frac{\ell_1 + \ell_2 + \ell_3}{Y} \right) \gamma_0, \end{aligned} \quad (128c)$$

$$N_{G_{ij}}^{(2)} = 1 - \frac{3b}{\sqrt{\beta_0}} \left(\frac{5}{2} - \frac{|\ln(x_1 x_2 x_3)|}{\ln(Q/Q_0)} \right) \frac{1}{\sqrt{\ln(Q/Q_0)}} = 1 - 3b \left(\frac{5}{2} - \frac{\ell_1 + \ell_2 + \ell_3}{Y} \right) \gamma_0, \quad (128d)$$

$$C_{G_{ij}}^{(2)} = 1 + \frac{1 - \frac{b}{\sqrt{\beta_0}} \left(5 - 3 \frac{|\ln(x_i x_j)|}{\ln(Q/Q_0)} \right) \frac{1}{\sqrt{\ln(Q/Q_0)}}}{3 + 9 \left[\frac{\ln(x_i/x_j)}{\ln(Q/Q_0)} \right]^2 - 2 \sqrt{\frac{\beta_0}{\ln(Q/Q_0)}} - \frac{a}{\sqrt{\beta_0}} \left(5 - 3 \frac{|\ln(x_i x_j)|}{\ln(Q/Q_0)} \right) \frac{1}{\sqrt{\ln(Q/Q_0)}}}, \quad (128e)$$

$$= 1 + \frac{1 - b \left(5 - 3 \frac{\ell_i + \ell_j}{Y} \right) \gamma_0}{3 + 9 \left(\frac{\ell_i - \ell_j}{Y} \right)^2 - 2 \beta_0 \gamma_0 - a \left(5 - 3 \frac{\ell_i + \ell_j}{Y} \right) \gamma_0}, \quad (128f)$$

$$C_{Q_{ij}}^{(2)} = 1 + \frac{N_c}{C_F} \left[C_{G_{ij}}^{(2)} - 1 + \frac{1}{4} (b - a) \gamma_0 \left(5 - 3 \frac{|\ln x_i x_j|}{\sqrt{\ln(Q/Q_0)}} \right) \right] \quad (128g)$$

$$= 1 + \frac{N_c}{C_F} \left[C_{G_{ij}}^{(2)} - 1 + \frac{1}{4} (b - a) \gamma_0 \left(5 - 3 \frac{\ell_i + \ell_j}{Y} \right) \right],$$

$$D_Q^{(3)} = 9 + 9 \left[\frac{\ln(x_2/x_1)}{\ln(Q/Q_0)} \right]^2 + 9 \left[\frac{\ln(x_3/x_1)}{\ln(Q/Q_0)} \right]^2 + 9 \left[\frac{\ln(x_3/x_2)}{\ln(Q/Q_0)} \right]^2 - \frac{6\beta_0}{\sqrt{\beta_0 \ln(Q/Q_0)}} \quad (128h)$$

$$- \frac{9a}{\sqrt{\beta_0}} \left(\frac{5}{2} - \frac{|\ln(x_1 x_2 x_3)|}{\ln(Q/Q_0)} \right) \frac{1}{\sqrt{\ln(Q/Q_0)}},$$

$$= 9 + 9 \left(\frac{\ell_1 - \ell_2}{Y} \right)^2 + 9 \left(\frac{\ell_1 - \ell_3}{Y} \right)^2 + 9 \left(\frac{\ell_2 - \ell_3}{Y} \right)^2 - 6\beta_0 \gamma_0 - 9a \left(\frac{5}{2} - \frac{\ell_1 + \ell_2 + \ell_3}{Y} \right) \gamma_0, \quad (128i)$$

$$N_Q^{(3)} = \frac{N_c^2}{C_F^2} C_{G_{123}}^{(3)} \left[1 - \frac{3a}{\sqrt{\beta_0}} \left(\frac{5}{2} - \frac{|\ln(x_1 x_2 x_3)|}{\ln(Q/Q_0)} \right) \frac{1}{\sqrt{\ln(Q/Q_0)}} \right] \quad (128j)$$

$$= \frac{N_c^2}{C_F^2} C_{G_{123}}^{(3)} \left[1 - \frac{3a}{\sqrt{\beta_0}} \left(\frac{5}{2} - \frac{\ell_1 + \ell_2 + \ell_3}{\ln(Q/Q_0)} \right) \frac{1}{\sqrt{\ln(Q/Q_0)}} \right].$$

D DLA solution of the 4-particle correlations

Below, we display the expressions related to subsection 2.9. In the l.h.s. of the evolution equation (69), we define

$$\begin{aligned} \hat{A}_{1234}^{(4)} &= A_{1234}^{(4)} - \left(A_{123}^{(3)} - A_1 A_2 A_3 \right) A_4 - \left(A_{134}^{(3)} - A_1 A_3 A_4 \right) A_2 - \left(A_{234}^{(3)} - A_2 A_3 A_4 \right) A_1 \\ &\quad - \left(A_{124}^{(3)} - A_1 A_2 A_4 \right) A_3 - \left(A_{12}^{(2)} - A_1 A_2 \right) \left(A_{34}^{(2)} - A_3 A_4 \right) - \left(A_{13}^{(2)} - A_1 A_3 \right) \left(A_{24}^{(2)} - A_2 A_4 \right) \\ &\quad - \left(A_{14}^{(2)} - A_1 A_4 \right) \left(A_{23}^{(2)} - A_2 A_3 \right) + \left(A_{12}^{(2)} - A_1 A_2 \right) A_3 A_4 + \left(A_{13}^{(2)} - A_1 A_3 \right) A_2 A_4 \\ &\quad + \left(A_{14}^{(2)} - A_1 A_4 \right) A_2 A_3 + \left(A_{23}^{(2)} - A_2 A_3 \right) A_1 A_4 + \left(A_{24}^{(2)} - A_2 A_4 \right) A_1 A_3 \\ &\quad + \left(A_{34}^{(2)} - A_3 A_4 \right) A_1 A_2 - A_1 A_2 A_3 A_4. \end{aligned} \quad (129)$$

In the DLA solution (70) of the equation (69), we have introduced the expressions:

$$H_1 = \left(\dot{C}_{12}^{(2)} - 1 \right) + \left(\dot{C}_{13}^{(2)} - 1 \right) + \left(\dot{C}_{14}^{(2)} - 1 \right) + \left(\dot{C}_{23}^{(2)} - 1 \right) + \left(\dot{C}_{24}^{(2)} - 1 \right) + \left(\dot{C}_{34}^{(2)} - 1 \right), \quad (130)$$

$$\begin{aligned} H_2 &= \left(\dot{C}_{123}^{(3)} - 1 \right) + \left(\dot{C}_{124}^{(3)} - 1 \right) + \left(\dot{C}_{134}^{(3)} - 1 \right) + \left(\dot{C}_{234}^{(3)} - 1 \right) + \left(\dot{C}_{14}^{(2)} - 1 \right) \left(\dot{C}_{23}^{(2)} - 1 \right) \\ &\quad + \left(\dot{C}_{34}^{(2)} - 1 \right) \left(\dot{C}_{12}^{(2)} - 1 \right) + \left(\dot{C}_{13}^{(2)} - 1 \right) \left(\dot{C}_{24}^{(2)} - 1 \right) - 2 \left(\dot{C}_{12}^{(2)} - 1 \right) - 2 \left(\dot{C}_{13}^{(2)} - 1 \right) \\ &\quad - 2 \left(\dot{C}_{14}^{(2)} - 1 \right) - 2 \left(\dot{C}_{23}^{(2)} - 1 \right) - 2 \left(\dot{C}_{24}^{(2)} - 1 \right) - 2 \left(\dot{C}_{34}^{(2)} - 1 \right), \end{aligned} \quad (131)$$

$$\begin{aligned}
H_3 = & 1 + \left(\dot{c}_{123}^{(3)} - 1\right) + \left(\dot{c}_{124}^{(3)} - 1\right) + \left(\dot{c}_{134}^{(3)} - 1\right) + \left(\dot{c}_{234}^{(3)} - 1\right) + \left(\dot{c}_{14}^{(2)} - 1\right) \left(\dot{c}_{23}^{(2)} - 1\right) \\
& + \left(\dot{c}_{34}^{(2)} - 1\right) \left(\dot{c}_{12}^{(2)} - 1\right) + \left(\dot{c}_{13}^{(2)} - 1\right) \left(\dot{c}_{24}^{(2)} - 1\right) - \left(\dot{c}_{12}^{(2)} - 1\right) - \left(\dot{c}_{13}^{(2)} - 1\right) \\
& - \left(\dot{c}_{14}^{(2)} - 1\right) - \left(\dot{c}_{23}^{(2)} - 1\right) - \left(\dot{c}_{24}^{(2)} - 1\right) - \left(\dot{c}_{34}^{(2)} - 1\right).
\end{aligned} \tag{132}$$

References

- [1] Redamy Perez Ramos, Vincent Mathieu, and Miguel-Angel Sanchis-Lozano. Three-particle correlations in QCD parton showers. arXiv:1104.1973 [hep-ph].
- [2] Harald Fritzsch and Murray Gell-Mann. Current algebra: Quarks and what else? *eConf*, C720906V2:135–165, 1972.
- [3] D. J. Gross and Frank Wilczek. ULTRAVIOLET BEHAVIOR OF NON-ABELIAN GAUGE THEORIES. *Phys. Rev. Lett.*, 30:1343–1346, 1973.
- [4] G. Hanson et al. Evidence for Jet Structure in Hadron Production by $e^+ e^-$ Annihilation. *Phys. Rev. Lett.*, 35:1609–1612, 1975.
- [5] Christoph Berger et al. JET ANALYSIS OF THE UPSILON (9.46) DECAY INTO CHARGED HADRONS. *Phys. Lett.*, B82:449, 1979.
- [6] Yuri L. Dokshitzer, Valery A. Khoze, Alfred H. Mueller, and S. I. Troian. Gif-sur-Yvette, France: Ed. Frontieres (1991) 274 p. (Basics of).
- [7] Yakov I. Azimov, Yuri L. Dokshitzer, Valery A. Khoze, and S. I. Troyan. Similarity of Parton and Hadron Spectra in QCD Jets. *Z. Phys.*, C27:65–72, 1985.
- [8] Yakov I. Azimov, Yuri L. Dokshitzer, Valery A. Khoze, and S. I. Troyan. Humpbacked QCD Plateau in Hadron Spectra. *Zeit. Phys.*, C31:213, 1986.
- [9] M. Z. Akrawy et al. A Study of coherence of soft gluons in hadron jets. *Phys. Lett.*, B247:617–628, 1990.
- [10] G. Abbiendi et al. Intermittency and correlations in hadronic Z^0 decays. *Eur. Phys. J.*, C11:239–250, 1999.
- [11] T. Aaltonen et al. Two-Particle Momentum Correlations in Jets Produced in $p\bar{p}$ Collisions at $\sqrt{s} = 1.96$ -TeV. *Phys. Rev.*, D77:092001, 2008.
- [12] T. Aaltonen et al. Measurement of the k_T Distribution of Particles in Jets Produced in $p\bar{p}$ Collisions at $\sqrt{s} = 1.96$ -TeV. *Phys. Rev. Lett.*, 102:232002, 2009.
- [13] Redamy Perez-Ramos and Bruno Machet. MLLA inclusive hadronic distributions inside one jet at high energy colliders. *JHEP*, 04:043, 2006.

- [14] Redamy Pérez Ramos, Francois Arleo, and Bruno Machet. Next-to-MLLA corrections to single inclusive kt- distributions and 2-particle correlations in a jet. *Phys. Rev.*, D78:014019, 2008.
- [15] Francois Arleo, Redamy Pérez Ramos, and Bruno Machet. Hadronic single inclusive kt distributions inside one jet beyond MLLA. *Phys. Rev. Lett.*, 100:052002, 2008.
- [16] Yuri L. Dokshitzer, Victor S. Fadin, and Valery A. Khoze. On the Sensitivity of the Inclusive Distributions in Parton Jets to the Coherence Effects in QCD Gluon Cascades. *Z. Phys.*, C18:37, 1983.
- [17] C. P. Fong and B. R. Webber. TWO PARTICLE CORRELATIONS AT SMALL x IN QCD JETS. *Phys. Lett.*, B241:255, 1990.
- [18] C. P. Fong and B. R. Webber. One and two particle distributions at small x in QCD jets. *Nucl. Phys.*, B355:54–81, 1991.
- [19] Redamy Perez Ramos. Two particle correlations inside one jet at 'modified leading logarithmic approximation' of quantum chromodynamics. I: Exact solution of the evolution equations at small x . *JHEP*, 06:019, 2006.
- [20] P. D. Acton et al. A Study of two particle momentum correlations in hadronic Z^0 decays. *Phys. Lett.*, B287:401–412, 1992.
- [21] E. A. De Wolf, I. M. Dremin, and W. Kittel. Scaling laws for density correlations and fluctuations in multiparticle dynamics. *Phys. Rept.*, 270:1–141, 1996.
- [22] W. Kittel and E. A. De Wolf. Soft multihadron dynamics. Hackensack, USA: World Scientific (2005) 652 p.
- [23] K. Konishi, A. Ukawa, and G. Veneziano. Jet Calculus: A Simple Algorithm for Resolving QCD Jets. *Nucl. Phys.*, B157:45–107, 1979.
- [24] Yuri L. Dokshitzer, Dmitri Diakonov, and S. I. Troian. Hard Processes in Quantum Chromodynamics. *Phys. Rept.*, 58:269–395, 1980.
- [25] Redamy Perez Ramos. Single inclusive distribution and two-particle correlations inside one jet at 'modified leading logarithmic approximation' of quantum chromodynamics. II: Steepest descent evaluation at small X . *JHEP*, 09:014, 2006.
- [26] Yuri L. Dokshitzer, Valery A. Khoze, and S. I. Troian. COHERENCE AND PHYSICS OF QCD JETS. *Adv. Ser. Direct. High Energy Phys.*, 5:241–410, 1988.
- [27] Yuri L. Dokshitzer, Victor S. Fadin, and Valery A. Khoze. Double Logs of Perturbative QCD for Parton Jets and Soft Hadron Spectra. *Zeit. Phys.*, C15:325, 1982.
- [28] Valery A. Khoze and Wolfgang Ochs. Perturbative QCD approach to multiparticle production. *Int. J. Mod. Phys.*, A12:2949–3120, 1997.
- [29] V. S. Fadin. Double logarithmic asymptotics of the cross-sections of $e^+ e^-$ annihilation into quarks and gluons. *Sov. J. Nucl. Phys.*, 37:245, 1983.

- [30] Z. Koba, Holger Bech Nielsen, and P. Olesen. Scaling of multiplicity distributions in high-energy hadron collisions. *Nucl. Phys.*, B40:317–334, 1972.
- [31] Yuri L. Dokshitzer. Improved QCD treatment of the KNO phenomenon. *Phys. Lett.*, B305:295–301, 1993.
- [32] E. D. Malaza and B. R. Webber. MULTIPLICITY DISTRIBUTIONS IN QUARK AND GLUON JETS. *Nucl. Phys.*, B267:702, 1986.
- [33] Sergio Lupia, Wolfgang Ochs, and Jacek Wosiek. Poissonian limit of soft gluon multiplicity. *Nucl. Phys.*, B540:405–433, 1999.
- [34] S. Chekanov et al. Multiplicity moments in deep inelastic scattering at HERA. *Phys. Lett.*, B510:36–54, 2001.
- [35] G. Abbiendi et al. QCD coherence and correlations of particles with restricted momenta in hadronic Z decays. *Phys. Lett.*, B638:30–38, 2006.